Molecular Cell *22*, 363–374, May 5, 2006 ©2006 Elsevier Inc. DOI 10.1016/j.molcel.2006.03.025

The Structure of the yFACT Pob3-M Domain, Its Interaction with the DNA Replication Factor RPA, and a Potential Role in Nucleosome Deposition

Andrew P. VanDemark,[1] Mary Blanksma,[1] Elliott Ferris,[1] Annie Heroux,[2] Christopher P. Hill,[1,*] and Tim Formosa[1,*]

[1] Department of Biochemistry
University of Utah School of Medicine
Salt Lake City, Utah 84132

[2] Biology Department
Brookhaven National Laboratory
Upton, New York 11973

Summary

We report the crystal structure of the middle domain of the Pob3 subunit (Pob3-M) of *S. cerevisiae* FACT (yFACT, *fa*cilitates *c*hromatin *t*ranscription), which unexpectedly adopts an unusual double pleckstrin homology (PH) architecture. A mutation within a conserved surface cluster in this domain causes a defect in DNA replication that is suppressed by mutation of replication protein A (RPA). The nucleosome reorganizer yFACT therefore interacts in a physiologically important way with the central single-strand DNA (ssDNA) binding factor RPA to promote a step in DNA replication. Purified yFACT and RPA display a weak direct physical interaction, although the genetic suppression is not explained by simple changes in affinity between the purified proteins. Further genetic analysis suggests that coordinated function by yFACT and RPA is important during nucleosome deposition. These results support the model that the FACT family has an essential role in constructing nucleosomes during DNA replication, and suggest that RPA contributes to this process.

Introduction

FACT (*fa*cilitates *c*hromatin *t*ranscription) is an essential chromatin reorganizing factor (Belotserkovskaya and Reinberg, 2004; Formosa, 2002; O'Donnell et al., 2004). The complex from the yeast *S. cerevisiae*, yFACT, is composed of three proteins: Spt16/Cdc68 (120 kDa), Pob3 (63 kDa), and Nhp6 (11 kDa). FACT subunits are highly conserved among eukaryotes, although in metazoans the Pob3 and Nhp6 orthologs are fused to form SSRP1. Of these components, only the structure of the nonspecific DNA binding protein Nhp6 has been reported (Allain et al., 1999; Masse et al., 2002).

Purified yFACT increases the accessibility of some nucleosomal DNA sites to nucleases (Formosa et al., 2001; Rhoades et al., 2004; Ruone et al., 2003). In contrast to ATP-dependent chromatin remodeling factors (Langst and Becker, 2004; Vignali et al., 2000), yFACT enhances digestion of nucleosomal DNA without translocating histone octamers to expose the affected sites and without hydrolyzing ATP (Orphanides et al., 1998; Rhoades et al., 2004; Ruone et al., 2003). Although the physical state of the nucleosomes altered by yFACT remains speculative, we have called the activity of yFACT "reorganization" to distinguish it from remodeling.

FACT has at least two important roles in transcription. First, yFACT promotes normal initiation. Mutation of *SPT16* or *POB3* or overexpression of *SPT16* causes the Spt$^-$ phenotype, which results from abnormal transcription initiation site selection (Formosa et al., 2002; Malone et al., 1991; Rowley et al., 1991; Schlesinger and Formosa, 2000). Consistent with a direct role in initiation, yFACT enhances the otherwise inefficient interaction between TATA binding protein (TBP) and TFIIA with a nucleosomal TATA site both in vitro and in vivo (Biswas et al., 2005). Second, FACT promotes normal elongation of transcription by RNA polymerase II on chromatin templates in vitro; this activity was used to purify human FACT (Orphanides et al., 1998, 1999). FACT also associates with RNA Pol II complexes throughout transcribed regions in yeast and plants (Kim et al., 2004; Mason and Struhl, 2003; Duroux et al., 2004) and colocalizes with RNA Pol II in flies (Saunders et al., 2003). Also consistent with a role in elongation, some *spt16* mutations cause sensitivity to 6-azauracil, which perturbs rNTP pool balance and inhibits elongation (Formosa et al., 2002; John et al., 2000; Orphanides et al., 1999). yFACT subunits also display a range of physical and genetic interactions with other transcription initiation and elongation factors (Costa and Arndt, 2000; Formosa et al., 2002; Krogan et al., 2002; Shimojima et al., 2003; Squazzo et al., 2002), suggesting that FACT performs several different functions by interacting with multiple complexes.

In addition to these roles in transcription, FACT is also required for DNA replication. yFACT binds directly to DNA polymerase (Pol) α/primase, and yFACT subunits interact genetically with several replication factors (Budd et al., 2005; Formosa et al., 2002; Schlesinger and Formosa, 2000; Wittmeyer and Formosa, 1997; Wittmeyer et al., 1999; Zhou and Wang, 2004). A subset of *SPT16* and *POB3* mutations causes sensitivity to hydroxyurea (HU; Formosa et al., 2002; Schlesinger and Formosa, 2000; O'Donnell et al., 2004), which inhibits ribonucleotide reductase activity, decreasing dNTP production and thus interfering with DNA synthesis. *POB3* mutations that caused HU sensitivity also delayed S phase progression and made cells more dependent on the S phase checkpoint mediated by Mec1 (Schlesinger and Formosa, 2000). Further, FACT is needed for normal levels of DNA replication in frog oocyte extracts (Okuhara et al., 1999), and it is associated with DNA replication foci in mouse cells (Hertel et al., 1999).

The broad range of FACT functions can be explained by the need to overcome the inhibitory effects of nucleosomes at many steps during chromatin-based processes. In this view, reorganization of nucleosomes by FACT provides access to blocked DNA sites without requiring nucleosomal translocation. Alternatively, FACT could be responsible for promoting the formation of stable nucleosomes, and mutated FACT could cause deposition of defective nucleosomes during replication or

*Correspondence: chris@biochem.utah.edu (C.P.H.); tim@biochem.utah.edu (T.F.)

during transcriptional repression, leading to abnormal behavior of the resulting chromatin. A role for FACT in nucleosome deposition is consistent with several observations. First, purified human FACT has been shown to promote the assembly of nucleosomes in vitro (Belotserkovskaya et al., 2003). Second, inappropriate transcriptional initiation from cryptic promoters in some yFACT mutants has been interpreted as a failure to reform normal chromatin after passage of RNA polymerase II (Kaplan et al., 2003). Third, some yFACT mutations are lethal when combined with mutations in the Hir/Hpc complex, indicating greater reliance on a pathway that has been implicated in nucleosome deposition (Formosa et al., 2002). These two views of FACT function, relieving nucleosomal inhibition and promoting nucleosome assembly, are not incompatible, as both could arise from an ability to chaperone nucleosomal components or to interconvert intermediates.

Here we report the crystal structure of the middle domain of Pob3 (Pob3-M). Unexpectedly, Pob3-M has an unusual "double PH" domain architecture. Conserved residues cluster on one face of the structure, indicating a surface that is functionally important. Genetic analysis indicates that this surface functions in DNA replication in a process that also involves the ssDNA binding factor replication protein A (RPA). The responses of the yFACT and RPA mutants to manipulations of histone genes suggest that yFACT and RPA cooperate to promote nucleosome deposition during DNA replication.

Results and Discussion

Structural Domains of Spt16-Pob3

We characterized the domain structure of yFACT by subjecting purified Spt16-Pob3 to limited proteolysis (Figure 1 and see Figures S1A and S1B in the Supplemental Data available with this article online). These results guided expression of various domains either individually or in combination to determine which were soluble and which were involved in the Spt16-Pob3 dimer interface (Figure S1C). This analysis indicated that Spt16 is composed of four domains (Figure 1): N terminal (N, similar in sequence with a family of aminopeptidases; Ponting, 2002), dimerization (D), middle (M), and C terminal (C). Pob3 is composed of three domains: N terminal and dimerization (N/D), middle (M), and C terminal (C). Similar results based on partial proteolysis have been reported previously (O'Donnell et al., 2004). The involvement of the N/D domain of Pob3 in dimerization with Spt16 is consistent with studies of human FACT (Keller and Lu, 2002). The C-terminal domains of each protein have high fractions of acidic residues and are predicted to be largely unstructured. Genetic analysis suggested that Pob3-M has a specific role in DNA replication (see below), so we initially focused on the structure of this domain.

Pob3-M Adopts a Double PH Domain Structure

Pob3-M was purified and crystallized. Phases were estimated by the SAD method from a selenomethionine-substituted variant protein in which leucines 297, 298, and 300 were replaced with methionines. The structure was refined to an R factor/R_{free} of 20.8%/26.9% against 2.2 Å data (Table 1). Residues 237–424 and 434–474 are ordered in the structure, and the two independent

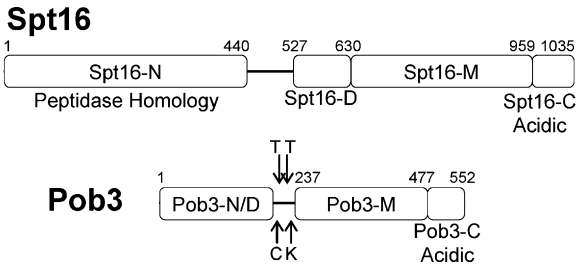

Figure 1. yFACT Domain Structure

Partial proteolysis and the solubility of singly or coexpressed fragments (Figure S1) were used to delineate structural domains of Spt16-Pob3, named as described in the text. Sites digested by trypsin (T), chymotrypsin (C), and proteinase K (K) are indicated for Pob3; other boundaries were defined as noted in Figure S1.

molecules in the asymmetric unit superimpose on each other with an rmsd of 0.7 Å for 237 pairs of ordered Cα atoms.

Pob3-M comprises two pleckstrin homology (PH) domain motifs (residues 248–367 and 383–474; Figure 2). This finding was unanticipated because, although the Pob3 sequence is conserved throughout eukaryotes (the SSRP1 family or pfam SSrecog; Marchler-Bauer et al., 2005; Marchler-Bauer and Bryant, 2004), sequence similarity with other proteins was not apparent. PH domain structures comprise a 7-stranded antiparallel β barrel that is capped at one end by a helix. The two Pob3-M PH domain structures are similar to each other (rmsd of 2.3 Å on 78 pairs of Cα atoms), and they each correspond closely to the standard PH domain motif. For example, Pob3 383–474 overlaps with one of the PH domains of pleckstrin (1PLS, Yoon et al., 1994) with an rmsd of 2.5 Å on 87 pairs of Cα atoms using the program DALI (Holm and Sander, 1998). In addition to the elements of a standard PH domain, Pob3-M 248–367 also contains two strands and a helix (S8, S9, and H2) that are inserted between the last strand of the PH domain (S7) and the β barrel-capping helix (H3), and two strands (S6′ and S6″) that contribute to the relatively long Q308 loop that is inserted between strands S6 and S7 (Figure 2).

Notably, the two PH domains are intimately associated with each other. They are related primarily by a translation such that their β barrels point in the same direction and the sides of the barrels pack against each other. A total of ~500 $Å^2$ of solvent-accessible surface area would be exposed if the two domains were separated from each other without other conformational changes. Further, numerous side chains that have been conserved as hydrophobic are buried in this interface (e.g., L288, F315, V317, Y396, L398, F403, and L405; see Figure S2). Thus, consistent with the limited proteolysis data, the Pob3-M domain should be viewed as one double PH domain rather than as two adjacent but relatively independent PH domains.

The many PH domain-like structures that have been observed belong to six distinct subgroups that each adopt the same overall fold but lack significant sequence similarity with one another (Marchler-Bauer et al., 2005; Marchler-Bauer and Bryant, 2004). The Pob3-M domain constitutes a seventh such subgroup. PH domains are best known as inositol lipid binding modules that function in regulated membrane binding, although this

Table 1. Data Collection and Refinement Statistics for the Pob-M and Pob3-M(Q308K) Structures

	Pob3-M	Pob3-M(Q308K)
Data Collection		
Space group	$P2_12_12_1$	$P2_1$
Unit cell dimensions (Å)	a = 57.11, b = 57.77, c = 157.58	a = 57.89, b = 157.53, c = 57.79 β = 89.7°
Resolution (Å)	50–2.21	40–2.55
Outer shell (Å)	2.29–2.21	2.64–2.55
Number of reflections		
Unique	26,598	31,027
Total	334,160	286,760
Mean $I/\sigma_{(I)}$	60.4 (30.1)	15.1 (2.01)
Completeness (%)	99.3 (96.3)	91.7 (92.8)
R_{sym} (%)[a]	6.1 (15.0)	8.5 (60.4)
Refinement		
R factor/R_{free} (%)[b,c]	20.8/26.9	22.0/30.3
Nonhydrogen atoms		
Total	4062	7652
Solvent	254	78
Rmsd from ideal geometry		
Bond lengths (Å)	0.013	0.013
Bond angles (°)	1.436	1.497
Average isotropic B values (Å^2)	41.4	40.7
Ramachandran plot, nonglycine residue in		
Most favorable region (%)	90.2	86.4
Additional allowed region (%)	9.1	12.7
Generous allowed region (%)	0.7	1.0
Disallowed region (%)	0.0	0.0

Values in parentheses correspond to those in the outer resolution shell.
[a] $R_{sym} = (|(\Sigma I - \langle I \rangle)|)/(\Sigma I)$, where <I> is the average intensity of multiple measurements.
[b] R factor = $\Sigma_{hkl}||F_{obs}(hkl)|| - F_{calc}(hkl)||/\Sigma_{hkl}|F_{obs}(hkl)|$.
[c] R_{free} = the crossvalidation R factor for 5% of reflections against which the model was not refined.

activity is limited to just one of the superfamily's subgroups (Jacobs et al., 1999; Lemmon, 2004). Other PH-like families are also associated with binding to specific ligands, but their ligands are diverse, including lipids, peptides containing phosphotyrosine, polyproline, and other peptides or proteins (Jacobs et al., 1999; Lemmon, 2004). The presence of a PH domain therefore suggests a binding function but does not indicate the nature of the ligand (Yu et al., 2004). Furthermore, several different regions of the PH-fold surface are used for ligand binding by the various subgroups, so it is not possible to propose a specific binding surface of Pob3-M solely on the basis of the PH domain architecture.

Previous sequence analysis suggested weak similarity between residues 4–104 and 374–475 of Pob3 (Ponting, 2002). Pob3 (374–475) forms a standard PH fold (Figure 2), so the N terminus of Pob3 might also adopt this architecture and could form another binding site. This organization is consistent with formation of multiple contacts between Pob3 and nucleosomes or members of other complexes.

A Conserved Pob3-M Surface Functions in DNA Replication

We aligned a diverse subset of the approximately 60 sequences of members of the Pob3/SSRP1 family (Altschul et al., 1997) and displayed the invariant residues on the Pob3-M structure (Figure 2 and Figures S2 and S3). Many of the invariant surface residues cluster in one patch (red in Figure 2). The equivalent region is the binding site for inositol phosphates in pleckstrin (Ferguson et al., 2000), and this region of the PH domain of moesin is the binding site for a peptide (Pearson et al., 2000). Therefore, at least some PH-fold domains use this surface as a ligand binding site, and the high degree of conservation suggests that this is a functionally important region of Pob3.

A genetic screen revealed a role for the conserved surface of Pob3-M in DNA replication. HU decreases the rate of dNTP synthesis, slowing DNA replication and increasing the risk of replication-fork stalling. Therefore, mutations in many replication factors that are required for elongation or for the checkpoint response to DNA damage cause HU sensitivity (Parsons et al., 2004). Mutations that physically destabilize Pob3 increase sensitivity to HU (Schlesinger and Formosa, 2000), but this relatively mild effect is probably due to a decrease in the total yFACT activity available in the cell. To identify regions of Pob3 specifically involved in DNA replication pathways, we randomly mutagenized the entire *POB3* gene and then sought mutants that were highly sensitive to HU but were able to grow at 37°C, indicating that the mutated Pob3 protein remained stable but was unable to perform some replication function. Twenty-three independent mutants of this type were obtained, and the *POB3* locus from each was sequenced. Surprisingly, while some isolates contained multiple mutations, all 23 mutants contained either a Q308R (14 isolates) or a Q308K (9 isolates) mutation in Pob3.

Q308 is within Pob3-M, surrounded by the highly conserved patch of residues noted above (Figures 2 and 3). It is located at the end of S6′, which together with S6″ forms a β ladder within a loop between strands S6 and S7 that is unusually long when compared with other PH domain folds (Figure 3). The main chain NH and CO groups of Q308 and T311 form hydrogen bonds, and the Q308 side chain is largely buried in a hydrophobic pocket. Although its orientation is not defined, one side chain N/O atom forms a hydrogen bond with the phenolic oxygen of the invariant residue Y257, and the other N/O atom is within 4.0 Å of the invariant P253 side chain and is exposed to solvent. This environment suggests that Q308 might affect the local conformation of the conserved surface patch in Pob3-M.

The *pob3-Q308K* mutation also causes the Spt$^-$ phenotype (indicated by growth on medium lacking lysine; see Figure 4), indicating diminished control of transcription. Importantly, the Q308K substitution does not cause Pob3 instability, as Western blot analysis indicates that protein levels are unchanged in mutant strains relative to the wild-type (Figure S4). Further, Pob3-Q308K forms a stable heterodimer with Spt16 (see below), and we have been able to purify and determine the structure of Pob3-M(Q308K) at a resolution of 2.5 Å (Table 1). The mutant protein is essentially indistinguishable from normal Pob3-M (rmsd of 0.8 Å over 220 Cα atoms), indicating that its effects in vivo are not caused by gross structural changes. Therefore, while Q308 is at the center of a highly conserved region of Pob3-M, the Q308K mutation does not destabilize Pob3 or Spt16, but it does

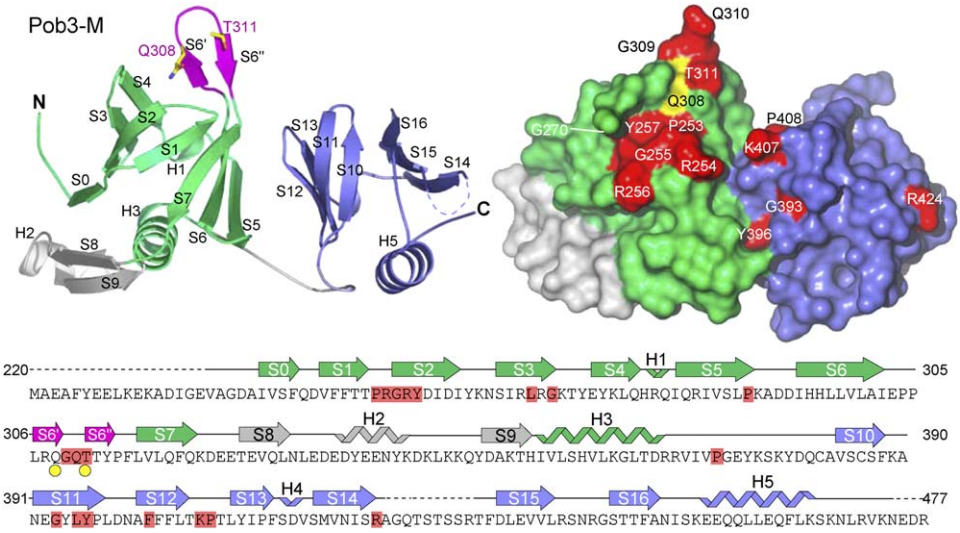

Figure 2. Structure of Pob3-M

(Left) Ribbon representation of Pob3-M. N-terminal (green) and C-terminal (blue) PH domains are shown. Strands S8, S9, and helix H2 (gray) are not found in a minimal PH fold. The loop between strands S6 and S7 (pink) is unusually long, includes two additional strands (S6′ and S6″), and contains residue Q308 (yellow). Disordered residues are modeled as dashed lines. (Right) A surface representation of Pob3-M in a similar orientation. Surface residues that are invariant in 12 Pob3/SSRP1 homologs (Figure S2) are colored red. Only two invariant surface residues are not visible in this view (Figure S3). Q308 (yellow) is highly conserved but not invariant (Figure S2). (Bottom) The Pob3-M sequence is shown with secondary structural elements. Invariant residues are shown on a red background. Q308 and T311 are indicated with yellow dots.

disturb the ability of yFACT to promote both normal transcription and normal DNA replication.

To further investigate the importance of Pob3-M, we mutated several highly conserved residues. This included changing residues T252, R254, R256, and D258 simultaneously to alanines; residues K271, T272, and Y273 to EAA; deleting Q308 and Q310 simultaneously; and mutating Q308 to alanine or aspartate. These changes caused very mild or no effects and in particular did not cause sensitivity to HU (Figure S5). The high degree of conservation observed in this region of the Pob3-M surface suggests that substitutions are detrimental on an evolutionary time scale, but our results show they are tolerated briefly under laboratory conditions. Yeast cells are therefore able to perform DNA replication, and to a lesser extent transcription, fairly well when the conserved surface patch in Pob3-M is modified, but not if a basic residue is substituted at position 308. If the conserved patch is a binding site with an important function in DNA replication, this pattern of responses to mutations suggests that the binding interaction includes multiple, partially redundant sites of contact.

pob3-Q308K Is Suppressed by an Intragenic Mutation

To analyze the physiological function disrupted by the Q308K mutation, we sought suppressors of the HU sensitivity. One HU-resistant strain was found to contain both the original Q308K mutation and a new T311A change within Pob3. T311 is highly conserved (Figure 2 and Figure S2) and forms two main chain hydrogen bonds with Q308. Notably, the *pob3-Q308K*, *T311A* double mutant is HU resistant but remains Spt$^-$ (Figure S6). The defect in DNA replication caused by *pob3-Q308K* can therefore be separated from the defect in transcription, indicating that both pathways use the conserved patch in Pob3-M but that their requirements differ.

Pob3-M Interacts Functionally with RPA

Analysis of one extragenic suppressor of the HU sensitivity caused by *pob3-Q308K* produced the surprising

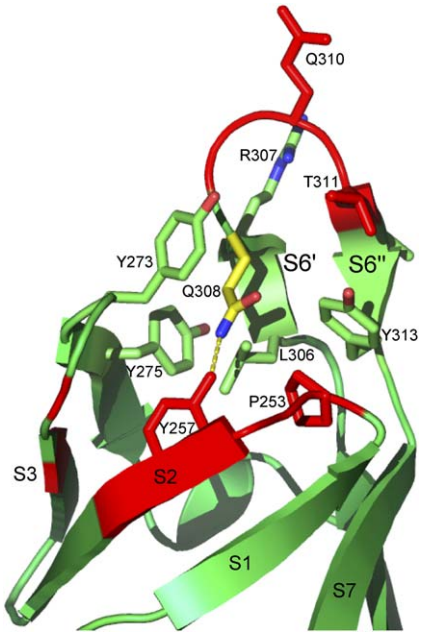

Figure 3. Close-up View of Q308 and Surrounding Residues

Residues within 5 Å of Q308 are shown in stick representation. Orientation is similar to Figure 2, and colors are the same as Figure 2. The H bond between the Q308 side chain and Y257 is shown as a dashed line.

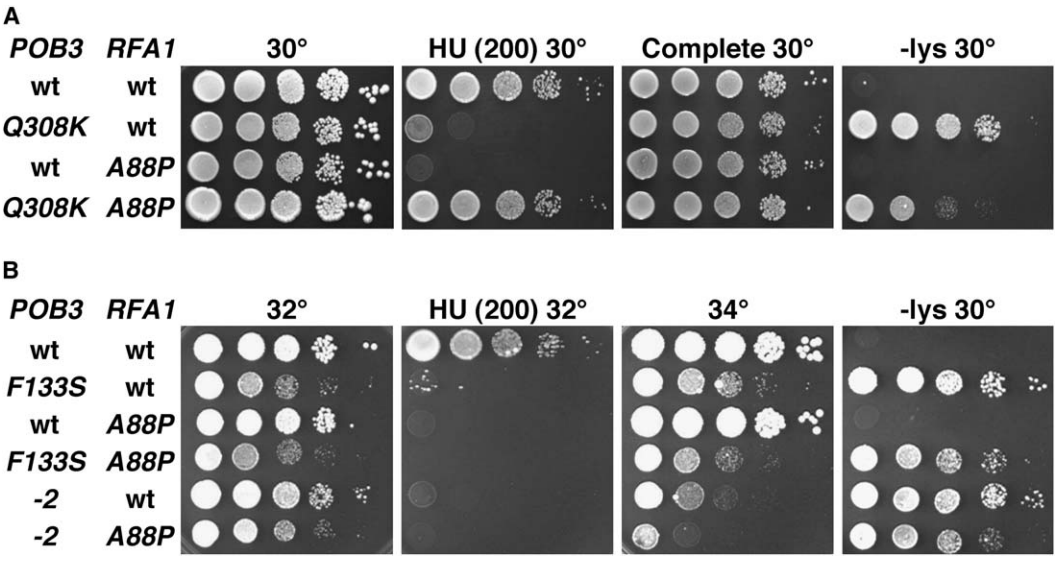

Figure 4. Genetic Analysis of *POB3* Mutations and Suppressors

(A) Aliquots of 10-fold dilutions of strains 8127-5-2, 8151-1-3, 8208-2-2, and 8208-7-3 (Table S1) were spotted and incubated as indicated. The leftmost panel is rich medium, HU (200) is rich medium plus 200 mM HU, Complete is synthetic medium, and −lys lacks lysine.

(B) As above, except that strains 8127-7-4, 8136-F133S, 8153-6-7a, 8212-3-2, 8213-4-1, and 8213-10-2 (Table S1) were used, and the left three panels are rich medium.

result that the suppressing mutation itself caused HU sensitivity. Thus, strains that have either the *pob3-Q308K* mutation or the suppressor mutation alone are HU sensitive, but a strain with both mutations is resistant. This pattern of mutual suppression can indicate that the two affected proteins cooperate to promote a similar function. Three lines of evidence show that the suppressing mutation is in *RFA1*, the gene that encodes the large subunit of the ssDNA binding factor RPA. First, a plasmid with only *RFA1* complemented the HU sensitivity caused by the suppressor mutation. Second, the suppressor mutation was mapped and found to be about 8 cM from *ADE1*, consistent with the physical distance of about 12 kbp between *RFA1* and *ADE1*. Third, the *RFA1* locus from wild-type and suppressor strains was found to differ at a single site, a G262C mutation leading to an A88P change. The *rfa1-A88P* mutation therefore causes HU sensitivity and also almost completely suppresses the HU sensitivity caused by *pob3-Q308K* (Figure 4).

RPA is an essential factor in multiple facets of DNA metabolism, including replication, recombination, and repair (Bell and Dutta, 2002; Binz et al., 2004; Brill and Stillman, 1991; Iftode et al., 1999). It accomplishes these various roles partly by binding preferentially to ssDNA and partly by binding to other replication factors, including DNA Pol α/primase (Bae et al., 2003; Braun et al., 1997; Dornreiter et al., 1992; Kim and Brill, 2001). RPA has four main DNA binding domains, but none of these are affected by the A88P mutation (Figure 5A). Instead, this region forms a discrete structural domain that has been implicated in DNA damage checkpoint signaling and in protein-protein interactions (Jacobs et al., 1999). For example, the N-terminal domain of human RFA1 binds to a region of p53 (Bochkareva et al., 2005). The site in human RFA1 that aligns with yeast Rfa1-A88 lies within a groove that contacts p53 (Bochkareva et al., 2005), consistent with the possibility that the A88P mutation disturbs a binding interaction.

Suppression of HU sensitivity by *rfa1-A88P* is allele specific. *pob3-F133S* and *pob3-2* each cause temperature sensitivity, HU sensitivity, and the Spt$^-$ phenotype, but none of these phenotypes were suppressed by *rfa1-A88P* (Figure 4). This specificity shows that *rfa1-A88P* does not suppress defects in Pob3 function by simply bypassing the need for yFACT function, as this would be expected to affect all *pob3* mutants. Instead, *rfa1-A88P* specifically ameliorates a defect caused by the *pob3-Q308K* mutation, suggesting restored functional cooperation between Pob3 and Rfa1 in a common process that is disturbed by each single mutation.

The *rfa1-A88P* mutation suppresses the HU sensitivity caused by *pob3-Q308K* to essentially wild-type levels (Figure 4) but has only a small effect on the Spt$^-$ phenotype (Figure 4; the double mutant remains significantly Lys$^+$ relative to the wild-type). We interpret this to mean that the Q308K mutation causes defects in both replication (HU sensitivity) and transcription (Spt$^-$), but only the replication defect is reversed by the *rfa1-A88P* mutation.

Pob3-M and RPA Interact Directly

A simple model to explain the phenotypes caused by *pob3-Q308K* and *rfa1-A88P* mutations is the following: the Pob3-M domain mediates yFACT-RPA binding, either mutation disrupts the binding, and the mutated proteins regain the ability to bind to one another. To test this model, we first determined whether purified yFACT and RPA could be coimmunoprecipitated in vitro. Antiserum generated against Pob3 protein precipitated RPA only if Spt16-Pob3 was present, showing that RPA interacts with Spt16-Pob3 (Figure 5B). In the reciprocal experiment, intact Spt16-Pob3 interacted nonspecifically with antibodies generated against Rfa1. This required

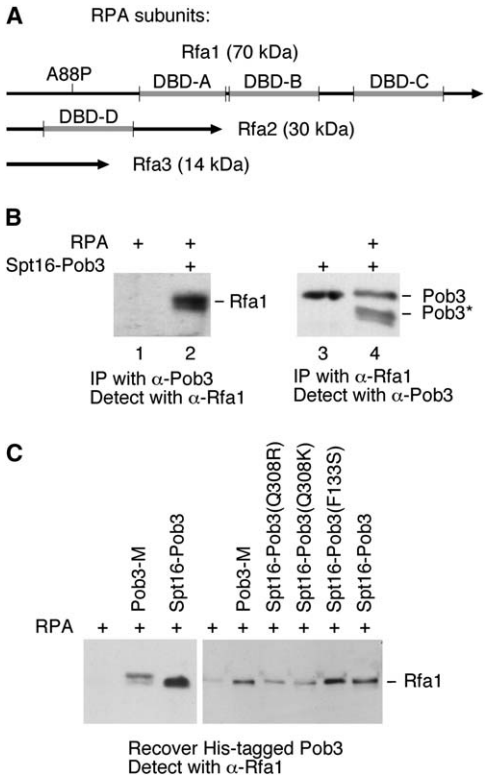

Figure 5. Physical Interaction between yFACT and RPA

(A) Schematic map of the three subunits of RPA with the location of the A88P mutation. The four highest affinity DNA binding domains are indicated (DBD-A, -B, -C, -D as in Bastin-Shanower and Brill [2001]).

(B) Purified RPA and Spt16-Pob3 were mixed as indicated, then immunoprecipitated with anti-Pob3 (left) or anti-Rfa1 antisera (right). Proteins from the IPs were separated by SDS-PAGE, blotted, then probed with antisera generated against Rfa1 (left) or Pob3 (right). Pob3* is a spontaneous proteolytic fragment of Pob3 lacking the C-terminal domain (T.F. and M.B., unpublished data).

(C) Purified RPA was mixed with no additional protein or equivalent amounts of (His_8)-Pob3-M or Spt16-(His_{12})-Pob3 with the mutations shown, then recovered with a chelated nickel matrix. Bound Rfa1 was eluted with SDS and detected with antisera after SDS-PAGE.

the acidic C-terminal domain of Pob3, as a spontaneous proteolytic fragment lacking this domain (Pob3*) was recovered with Rfa1 antiserum only if RPA was present, again showing direct interaction between Spt16-Pob3 and RPA (Figure 5B).

We next used chelated nickel chromatography with histidine-tagged versions of Pob3 to allow greater quantitation of the binding between Pob3 and Rfa1. As in the IP assay above, intact Spt16-(His_{12}-Pob3) and the His_8-Pob3-M domain alone were each able to specifically bind RPA (Figure 5C). Further, use of Pob3-Q308K/R mutant proteins in these assays appeared to decrease the recovery of RPA relative to normal Pob3 protein or a Pob3-F133S mutant that does not interact genetically with RPA (Figures 4 and 5C). These results and similar data obtained using a GST-Pob3 fusion (data not shown) are consistent with a direct interaction between the Pob3-M domain and RPA. However, quantitation of the interaction using an ELISA method did not yield simple binding curves and did not show significantly different binding responses between wild-type and mutant pairs of Pob3 and RPA (data not shown). Only a small fraction of the tagged Pob3 molecules were capable of binding RPA in these assays, and the isolated N-terminal domain of Rfa1 did not bind Pob3 (data not shown). These results are inconsistent with the simple model outlined above.

Taken together, the in vitro binding data support a direct interaction between purified Spt16-Pob3 and RPA, but they suggest that this interaction is weak or transient. The data do not support the model that the Pob3-M domain and the N-terminal domain of Rfa1 act as simple autonomous binding modules whose affinity is altered by the *pob3-Q308K* and *rfa1-A88P* mutations. The effects of these mutations therefore appear to be more complicated than just loss and recovery of affinity between single binding surfaces on each protein. Therefore, while a direct interaction may be important for cooperation between yFACT and RPA, neither the HU sensitivity caused by the single mutants nor the robust mutual genetic suppression appears to be a consequence of simple changes in the affinity of this interaction. Instead, the suppression may involve interactions between yFACT and RPA and other replication factors, posttranslational modifications missing from the purified proteins, or changes in protein conformation or dynamics that only occur in specific contexts, such as during S phase.

Effect of Histone Manipulations on *pob3-Q308K*

We next sought to determine whether the common replication function promoted by yFACT and RPA is related to the known activity of yFACT in altering the properties of nucleosomes. We previously reported that the defects caused by some *pob3* alleles can be partially suppressed by increasing the ratio of H2A-H2B to H3-H4, but these same cells could not tolerate mutations that blocked acetylation of the H4 tail at positions 8 and 16 (Formosa et al., 2002), sites often associated with transcriptional regulation (Zhang et al., 1998). A similar analysis of *pob3-Q308K* reveals properties more consistent with defective DNA replication. The *pob3-Q308K* strain is able to tolerate the H4-K8R, K16R mutations, but its growth is severely impaired by H4-K5R, K12R (Figure 6A; few cells without the wild-type plasmid are detected on FOA in row 6, and they grow slowly compared with the wild-type strain or plasmid in row 1). Importantly, these are the sites that are acetylated in newly deposited nucleosomes during replication (reviewed in Gunjan et al. [2005]). This synthetic defect therefore links the deficiency in *pob3-Q308K* mutants to a process that includes deposition of nucleosomes. Consistent with the importance of histone tail modifications, *pob3-Q308K* strains displayed strong synthetic growth defects when either a histone acetyltransferase (Gcn5) or a deacetylase (Rpd3) was lacking (Figure 7A).

pob3-Q308K strains also displayed growth defects when histone pools were altered by overexpression (Figure 6B; compare rows 6–8 with row 5 on 75 mM HU, a condition that is normally permissive for a *pob3-Q308K* strain). Notably, the synthetic defect was especially severe with overexpression of H2A-H2B copy 2 (Figure 6B, row 8). This is the only set of histone genes in yeast that is not transcriptionally repressed by the

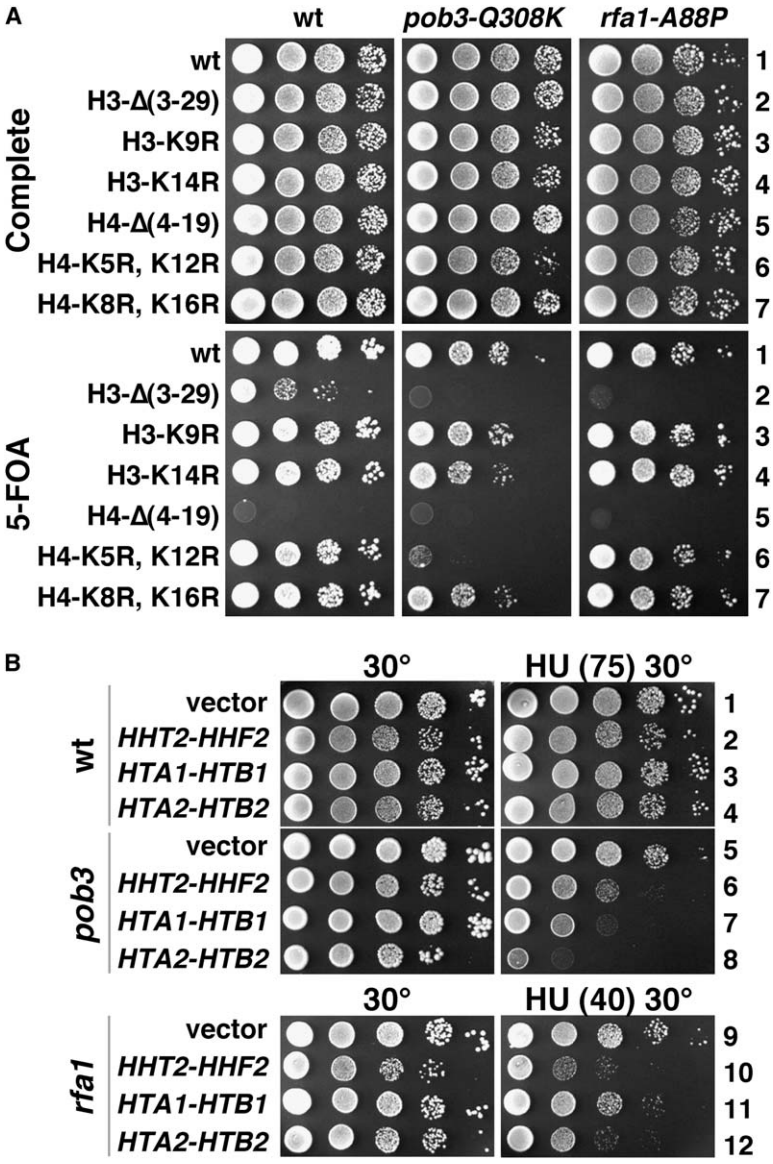

Figure 6. Effects of Histone Overexpression or Mutation

(A) Strains 8244-13-2, 8244-18-4, and 8239 (Table S1) carrying plasmid DS1700 (YCp *URA3 HHT2-HHF2*) were transformed with *TRP1*-marked plasmids with wild-type versions of both *HHT2* (histone H3) and *HHF2* (histone H4) or the mutation indicated (Zhang et al., 1998). Aliquots of 10-fold dilutions were placed on medium with or without 5-FOA at 30°C to select for cells lacking DS1700. Deletion of H4 (4–19) is lethal in this background (line 5).

(B) 8127-7-4, 8151-1-2, and 8208-7-2 (Table S1) were transformed with YEp352 (vector), DS4155 (YEp *HHT2-HHF2*), DS4543 (YEp *HTA1-HTB1*), and DS2824 (YEp *HTA2-HTB2*). Aliquots of 10-fold dilutions were placed on selective media at 30°C with or without HU (mM).

Hir/Hpc proteins (Recht et al., 1996) and is the condition that showed the most effective suppression of *pob3-7* (Formosa et al., 2002). Deletion of one copy of the genes that encode histones H3-H4 was also strongly detrimental in a *pob3-Q308K* strain (Figure 7), whereas decreased H3-H4 gene copy number had little effect on a *pob3-7* strain (Formosa et al., 2002). $(H3\text{-}H4)_2$ tetramers are the form initially deposited during nucleosome formation, so diminished tolerance of high ratios of H2A-H2B to H3-H4 in a *pob3-Q308K* strain underscores the distinct nature of this allele and is consistent with a defect in a step related to nucleosome deposition.

The CAF-1 complex promotes replication-dependent nucleosome deposition, and the Hir/Hpc complex promotes replication-independent deposition (reviewed in Gunjan et al., 2005). However, yeast cells lacking both CAF-1 and the Hir/Hpc complexes are viable, indicating that other deposition pathways must exist (Kaufman et al., 1998; Qian et al., 1998). If yFACT acts in such a pathway, then yFACT mutations that affect this process would be expected to display synthetic defects when paired with CAF-1 or Hir/Hpc mutations. Other *pob3* mutants tested were not affected by loss of CAF-1 (Formosa et al., 2002), but a *pob3-Q308K* mutant displayed moderately enhanced sensitivity to low levels of HU when the Rlf2 subunit of CAF-1 was deleted (Figures 7B and 7C; compare line 4 with line 3), consistent with overlapping functions. Combining *pob3-Q308K* with loss of the Hir/Hpc complex has more dramatic but less readily interpreted effects. A *pob3-Q308K hpc2-Δ* strain is inviable (data not shown), but this could be due to either of the two known functions of the Hir/Hpc complex: promoting replication-independent nucleosome deposition and regulating histone gene expression. *pob3-Q308K* could cause a defect in replication-dependent deposition and thereby make the replication-independent process essential. Alternatively, loss of repression by the Hir/Hpc complex causes both increased histone pool production and imbalanced histone pool production, which are each poorly tolerated by *pob3-Q308K* strains

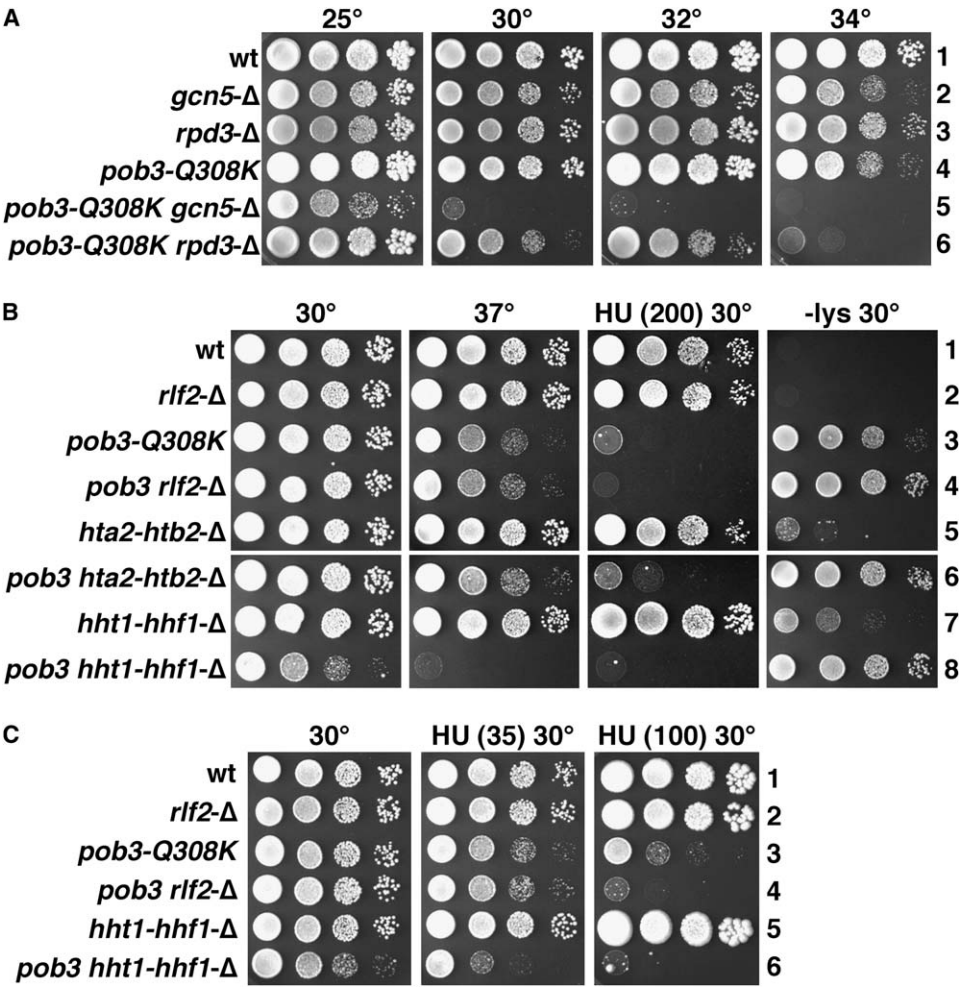

Figure 7. Genetic Interactions with *pob3-Q308K*

(A) Ten-fold dilutions of strains DY2861, 8230-9-2, 8230-2-1, 8224, 8230-2-4, and 8230-1-3 (Table S1) were spotted to rich medium and incubated as indicated. The Ts$^-$ caused by *pob3-L78R* is partially suppressed by *rpd3-Δ* (Formosa et al., 2001), but both *gcn5-Δ* and *rpd3-Δ* enhanced the growth defect caused by *pob3-Q308K* strains (compare lines 5 to 6 to lines 2–4).

(B and C) Dilutions of strains 8127-7-4, 8217-6-2, 8136-Q308K, 8217-2-1, 8218-2-4, 8218-3-3, 8219-3-3, and 8219-10-1 (Table S1) were spotted to rich medium with or without HU or on medium lacking lysine. Deletion of *RLF2/CAC1* (encoding the large subunit of CAF-1) did not cause HU sensitivity or the Spt$^-$ phenotype but enhanced both phenotypes caused by *pob3-Q308K* (weaker growth in [C], line 4 compared to line 3 with 100 mM HU, and stronger growth in [B], line 4 compared to line 3 on −lys). The Ts$^-$ caused by *pob3-7* is enhanced by an *hta2-htb2-Δ* mutation and suppressed by an *hht1-hhf1-Δ* mutation (Formosa et al., 2002). In contrast, a *pob3-Q308K* strain was unaffected by *hta2-htb2-Δ*, except for a slight enhancement of the Spt$^-$ phenotype (compare lines 6 and 3 on −lys), and displayed a strong synthetic defect with *hht1-hhf1-Δ* (compare lines 8 and 3 in [B] at 30ºC and 37ºC, and lines 6 and 3 in [C]).

(Figure 6B), and could also explain the observed synthetic lethality.

If RPA and yFACT cooperate to promote a common step in DNA replication, then *RFA1* should share some genetic interaction partners with *pob3-Q308K*. Like a *pob3-Q308K* strain but unlike wild-type, an *rfa1-A88P* strain was unable to tolerate deletion of the N-terminal tail of H3 (Figure 6A, row 2). Further, overexpression of either H3-H4 or H2A-H2B was detrimental to the *rfa1-A88P* mutant but not to a wild-type strain, resulting in increased HU sensitivity for the mutant (Figure 6B). These overlapping genetic interactions between the replication factor RPA and yFACT with histones are consistent with participation of both RPA and yFACT in a replication function involving histones, presumably nucleosome deposition.

Models of Pob3-M/yFACT Function

The structure of Pob3-M reveals a patch of highly conserved residues on a surface of a PH domain that is used for ligand binding in other proteins with this fold. A mutation within this patch leaves the protein stable but causes sensitivity to the DNA synthesis inhibitor HU and also causes abnormal transcription. These two defects can be separated genetically, and the activity related to HU sensitivity involves the function of the ssDNA binding factor RPA and also requires normal levels of histone proteins and the ability to modify histone H4 at the K5 and K12 positions. yFACT can interact directly with RPA, but it is not yet clear what role this binding plays in the collaboration between these factors. A yFACT mutation and an RPA mutation that each cause HU sensitivity separately result in no HU sensitivity when combined,

and each mutant is more sensitive to HU when histone levels are altered. We interpret these observations as evidence that yFACT and RPA cooperate to perform a step in DNA replication that involves nucleosome deposition, but other possibilities must be considered.

Effects of yFACT mutations on DNA replication might be indirectly caused by altered transcription. We consider this unlikely for the following reasons. First, the HU sensitivity and the transcription phenotype are genetically separable. If the HU sensitivity resulted from a defect in transcription, then suppression of the HU sensitivity would be accompanied by restoration of normal transcriptional regulation, but two of our suppressors do not have this property. Second, *pob3-Q308K* strains tolerate mutations in histone H4 that prevent normal acetylation at sites associated with transcription, but they do not tolerate mutation of sites associated with nucleosome deposition. If the replication defect were an indirect effect of altered transcription, further disturbance of transcription by mutations in K8 and K16 of H4 would amplify this effect more than mutations in K5 and K12 of H4, but the opposite was observed. Third, the properties of different alleles of *pob3* and their suppressors are not consistent with a strict transcription model. We have identified a variety of *POB3* and *SPT16* mutants by screening for temperature sensitivity (Formosa et al., 2002; Schlesinger and Formosa, 2000). Essentially all of the Ts^- alleles also caused the Spt^- phenotype, but only a small subset caused HU sensitivity. Importantly, the strengths of these phenotypes did not correlate with one another. If HU sensitivity resulted only from the most severe defects in transcription, then the alleles that cause HU sensitivity should also be those with the strongest Spt^- phenotype, but this is not the case. These observations do not rule out an indirect transcription model but are more consistent with our interpretation that the conserved patch in Pob3-M is important for both replication and transcription for independent reasons.

Another possible indirect explanation for the genetic interaction between yFACT and RPA is that it could involve checkpoint control. Yeast cells respond to HU by triggering a DNA damage checkpoint that uses RPA as a sensor and the protein kinases Mec1 and Rad53 as signal transducers, leading to induced transcription of DNA repair factors and ribonucleotide reductase, the target of HU inhibition (Zou and Elledge, 2003). *rfa1-A88P* cells could be sensitive to HU because they do not sense the damage, and *pob3-Q308K* cells could be sensitive to HU because they do not induce the transcriptional response. However, it is not obvious why these defects would suppress one another. One explanation is that the checkpoint response is somehow detrimental in *pob3-Q308K* cells and that *rfa1-A88P* rescues the cells by preventing checkpoint activation. Any other mutation in the checkpoint pathway should then also suppress, but we find that neither *rad53* nor *mec1* mutations have this effect (Figure S6). Instead, *rad53 pob3-Q308K* double mutants have a severe growth defect and display the same extreme sensitivity to HU as *rad53* single mutants (Figure S6). The *pob3-Q308K* mutation therefore does not suppress and is not suppressed by other checkpoint defects; instead, it causes increased dependence on the DNA damage checkpoint.

Our observations are more consistent with a direct role for yFACT in nucleosome deposition during replication, at a step that also involves the function of RPA. Direct binding observed between purified yFACT and RPA supports such a model, although the behavior of Rfa1-A88P and Pob3-Q308K proteins in binding assays does not conform to the predictions of a simple model in which the robust genetic suppression observed is due to restoration of disrupted binding affinity. This could indicate that the in vitro binding assays do not fully capture the in vivo context of the interaction, or that, instead of disturbing binding affinity, the mutations disrupt some function by altering the geometry or dynamics of binding. An attractive possibility is that yFACT and RPA interact through another factor, perhaps Polα/primase, which is known to bind directly to both yFACT and RPA (Braun et al., 1997; Dornreiter et al., 1992). Other candidates for a coordinating factor are suggested by the recent results linking yFACT to the GINS and MCM complexes, placing yFACT in a context central to the regulation of DNA replication (Gambus et al., 2006). The Pob3-M structure and the various mutant alleles of yFACT and RPA described here will be valuable tools for further dissecting the functional role or roles of these factors in promoting chromatin-dependent processes.

Experimental Procedures

Yeast Methods

Media, strains, and plasmids used are described in the Supplemental Data and in Table S1.

Protein Purification and Structure Determination

Yeast Pob3-M was expressed in *E. coli* Codon+ (RIL) cells (Stratagene) using a modified pET expression vector encoding an eight-residue, N-terminal histidine tag followed by a TEV protease cleavage site. TEV cleavage results in a protein whose N terminus is GHM, where the M is M220 of the native Pob3 sequence. Pob3-M was purified by nickel affinity chromatography (Qiagen) followed by an overnight digestion with TEV protease and a second round of nickel affinity chromatography to remove His-tagged TEV and any uncleaved Pob3-M. Cleaved Pob3-M was further purified by gel filtration on a Superdex-200 column (Pharmacia), with peak fractions eluting as an apparent monomer. Protein was concentrated to 15 mg/ml in 20 mM Tris-HCl (pH 7.5), 100 mM NaCl, 5% glycerol, 1 mM DTT using a Vivaspin concentrator (Millipore). The native sequence of Pob3-M contains only two methionine residues, including M220 at the extreme N terminus. To increase the potential anomalous signal, we mutated ^{297}LLVL^{300} to MMVM. Selenomethionine-substituted protein behaved like the native protein in both purification and crystallization.

Single plate-like crystals (300 × 150 × 40 μm) of Pob3-M were grown by the vapor-diffusion method in sitting drops using a reservoir solution containing 21% PEG 3350, 20% glycerol, 200 mM NaCl, 50 mM ammonium sulfate, 100 mM Tris-HCl (pH 7.5) over a period of 3 weeks. Single crystals were flash frozen directly from the mother liquor in liquid nitrogen. Initial diffraction quality was poor (~4 Å resolution with very high mosaicity) but was improved through successive rounds of crystal annealing. Annealing was performed by removing the looped crystal from the cryostream, allowing it to warm at room temperature for 1 min, then returning it to the cryostream. Most crystals only showed a modest improvement in diffraction quality, but occasionally crystals showed a marked improvement.

SAD data were collected at the NSLS beamline X26-C on a crystal of selenomethionine-substituted Pob3-M and were processed with DENZO and SCALEPACK (Otwinowski and Minor, 1996). The crystals belong to spacegroup $P2_12_12_1$ (a = 57.1, Å, b = 57.8, Å, c = 156.6 Å) and contain two molecules in the asymmetric unit. A total

of eight Se sites were located using SOLVE (Terwilliger and Berendzen, 1999), and an initial model was built into the experimental electron-density maps using RESOLVE (Terwilliger, 2003). Subsequent model building was carried out using COOT (Emsley and Cowtan, 2004), and refinement with TLS parameters was performed using REFMAC implemented in CCP4 (CCP4, 1994). TLS groups were generated using the TLSMD server (Painter and Merritt, 2006). Crystallographic statistics are given in Table 1.

Pob3-M(Q308K) was purified and crystallized using the same methods as for the wild-type protein. The crystals belonged to a related space group but, unlike wild-type, were not annealed prior to data collection. Initial phases were obtained via molecular replacement using Phaser implemented in CCP4 (CCP4, 1994) utilizing the wild-type structure as a search model. Refinement of the model against 2.55 Å data utilizing TLS parameters resulted in an R factorof 22.0% with an R_{free} of 30.3%. Despite the relatively high R_{free} values, simulated annealing omits show good agreement with the model.

Mutagenesis of Pob3 and Isolation of Suppressors

Primers that anneal about 200 bp outside of the *POB3* insert in plasmid pTF139 (Schlesinger and Formosa, 2000) were used to amplify the *POB3* gene using standard PCR conditions. Yeast strain 7787-4-4 pTF138, with a deletion of *POB3* but carrying a plasmid with the *URA3* and *POB3* genes, was transformed with a mixture of the PCR product and the vector YCplac111 (Gietz and Sugino, 1988) digested with HindIII and EcoRI. Leu^+ transformants were replica plated to medium containing 5-FOA to select cells that had lost the wild-type *POB3* plasmid, and then to medium lacking lysine to identify the 1%–5% of the colonies with the Spt^- phenotype, indicating a mutation in *POB3*. Due to this selection step, only mutants with the Spt^- phenotype were studied further in this screen. About 500 mutants were then screened for other phenotypes, including Ts^- and ability to grow on medium containing 200 mM HU. Twenty-three strains that were Ts^+ at 37ºC and tightly HU sensitive were chosen, the plasmids were isolated by transformation of bacteria, and the inserts were sequenced.

For integration into the genome, the *POB3* locus with the Q308K mutation was transferred from the pTF139 plasmid to a similar plasmid lacking an origin of replication and containing the *URA3* marker. This was integrated into the yeast genome, and then 5-FOA-resistant colonies that were HU sensitive were tested for popout of the plasmid, leaving behind the Q308K mutation in an otherwise unchanged cell. The *POB3* locus was amplified by PCR and sequenced to ensure accurate excision of the integrated plasmid. To isolate suppressors, aliquots of these cells were placed on medium containing 200 mM HU, and papillae with suppressing mutations were isolated for further analysis.

Immunoprecipitation and Nickel Chelation Pull-Downs

RPA was purified as described (Henricksen et al., 1994), and 10 ng (1 μM final concentration) was incubated for 1 hr at 4ºC in binding buffer (10 mM Tris-HCl [pH 7.5], 150 mM NaCl, 1 mM EDTA, and 0.3% Triton X-100), either with or without 16 ng (1 μM) of purified Spt16-Pob3 (Rhoades et al., 2004), in a final volume of 90 μl. One microliter of antiserum generated against purified Pob3 (Covance) was added and incubated with mixing for 1 hr at 4ºC. Ten microliters of a slurry of magnetic beads conjugated with protein A (New England Biolabs) was added and incubated with mixing for 1 hr at 4ºC, and then the beads were collected using a magnet. For nickel chelation, a similar protocol was used, except the antisera were omitted and the histidine-tagged Pob3 was recovered with HIS-Select HC Nickel magnetic beads (Sigma). The beads were washed four times, with 500 μl of binding buffer each time, and then bound proteins were eluted with SDS sample buffer for 5 min at 65ºC. Proteins were separated by SDS-PAGE, transferred to nitrocellulose (Schleicher and Schuell), blocked with 1% powdered milk in TBS-T (20 mM Tris-HCl [pH 7.5], 250 mM NaCl, 0.1% Tween-20), and then probed with antiserum generated against Rfa1 (Covance). Secondary antibody (goat anti-rabbit peroxidase conjugated, KPL) and ECL (Amersham Biosciences) were used to detect the Rfa1. Alternatively, Spt16-Pob3 was tested with or without added RPA using the same protocol as above, antiserum against Rfa1 was used for immunoprecipitation, and Pob3 was detected after SDS-PAGE.

Supplemental Data

Supplemental Data include six figures and one table and can be found with this article online at http://www.molecule.org/cgi/content/full/22/3/363/DC1/.

Acknowledgments

We thank Matthew Weber, Danny Gibbs, Susan Ruone, Amanda Butler, and Peter Winter for technical assistance; Bob Schackmann and the University of Utah Biotechnology Core Facility for N-terminal peptide sequencing; Sharon Dent and David Stillman for providing plasmids; and Brad Cairns, Jacqui Wittmeyer, and David Stillman for critical comments on this manuscript. Operations of the National Synchrotron Light Source (NSLS) are supported by the U.S. Department of Energy, Office of Basic Energy Sciences, and by the National Institutes of Health (NIH). Data collection at the NSLS was funded by the National Center for Research Resources. This work was supported by NIH grants GM076242 (C.P.H) and GM064649 (T.F.), and American Cancer Society grant PF0304001GMC (A.P.V.).

Received: August 24, 2005
Revised: January 10, 2006
Accepted: March 21, 2006
Published: May 4, 2006

References

Allain, F.H., Yen, Y.M., Masse, J.E., Schultze, P., Dieckmann, T., Johnson, R.C., and Feigon, J. (1999). Solution structure of the HMG protein NHP6A and its interaction with DNA reveals the structural determinants for non-sequence-specific binding. EMBO J. *18*, 2563–2579.

Altschul, S.F., Madden, T.L., Schaffer, A.A., Zhang, J., Zhang, Z., Miller, W., and Lipman, D.J. (1997). Gapped BLAST and PSI-BLAST: a new generation of protein database search programs. Nucleic Acids Res. *25*, 3389–3402.

Bae, K.H., Kim, H.S., Bae, S.H., Kang, H.Y., Brill, S., and Seo, Y.S. (2003). Bimodal interaction between replication-protein A and Dna2 is critical for Dna2 function both in vivo and in vitro. Nucleic Acids Res. *31*, 3006–3015.

Bastin-Shanower, S.A., and Brill, S.J. (2001). Functional analysis of the four DNA binding domains of replication protein A. The role of RPA2 in ssDNA binding. J. Biol. Chem. *276*, 36446–36453.

Bell, S.P., and Dutta, A. (2002). DNA replication in eukaryotic cells. Annu. Rev. Biochem. *71*, 333–374.

Belotserkovskaya, R., and Reinberg, D. (2004). Facts about FACT and transcript elongation through chromatin. Curr. Opin. Genet. Dev. *14*, 139–146.

Belotserkovskaya, R., Oh, S., Bondarenko, V.A., Orphanides, G., Studitsky, V.M., and Reinberg, D. (2003). FACT facilitates transcription-dependent nucleosome alteration. Science *301*, 1090–1093.

Binz, S.K., Sheehan, A.M., and Wold, M.S. (2004). Replication protein A phosphorylation and the cellular response to DNA damage. DNA Repair (Amst.) *3*, 1015–1024.

Biswas, D., Yu, Y., Prall, M., Formosa, T., and Stillman, D.J. (2005). The yeast FACT complex has a role in transcriptional initiation. Mol. Cell. Biol. *25*, 5812–5822.

Bochkareva, E., Kaustov, L., Ayed, A., Yi, G.S., Lu, Y., Pineda-Lucena, A., Liao, J.C., Okorokov, A.L., Milner, J., Arrowsmith, C.H., and Bochkarev, A. (2005). Single-stranded DNA mimicry in the p53 transactivation domain interaction with replication protein A. Proc. Natl. Acad. Sci. USA *102*, 15412–15417.

Braun, K.A., Lao, Y., He, Z., Ingles, C.J., and Wold, M.S. (1997). Role of protein-protein interactions in the function of replication protein A (RPA): RPA modulates the activity of DNA polymerase α by multiple mechanisms. Biochemistry *36*, 8443–8454.

Brill, S.J., and Stillman, B. (1991). Replication factor-A from Saccharomyces cerevisiae is encoded by three essential genes coordinately expressed at S phase. Genes Dev. *5*, 1589–1600.

Budd, M.E., Tong, A.H., Polaczek, P., Peng, X., Boone, C., and Campbell, J.L. (2005). A network of multi-tasking proteins at the

DNA replication fork preserves genome stability. PLoS Genet. *1*, e61 10.1371/journal.pgen.0010061.

CCP4 (Collaborative Computational Project, Number 4) (1994). The CCP4 suite: programs for protein crystallography. Acta Crystallogr. D Biol. Crystallogr. *50*, 760–763.

Costa, P.J., and Arndt, K.M. (2000). Synthetic lethal interactions suggest a role for the *Saccharomyces cerevisiae* rtf1 protein in transcription elongation. Genetics *156*, 535–547.

Dornreiter, I., Erdile, L.F., Gilbert, I.U., von Winkler, D., Kelly, T.J., and Fanning, E. (1992). Interaction of DNA polymerase alpha-primase with cellular replication protein A and SV40 T antigen. EMBO J. *11*, 769–776.

Duroux, M., Houben, A., Ruzicka, K., Friml, J., and Grasser, K.D. (2004). The chromatin remodelling complex FACT associates with actively transcribed regions of the Arabidopsis genome. Plant J. *40*, 660–671.

Emsley, P., and Cowtan, K. (2004). Coot: model-building tools for molecular graphics. Acta Crystallogr. D Biol. Crystallogr. *60*, 2126–2132.

Ferguson, K.M., Kavran, J.M., Sankaran, V.G., Fournier, E., Isakoff, S.J., Skolnik, E.Y., and Lemmon, M.A. (2000). Structural basis for discrimination of 3-phosphoinositides by pleckstrin homology domains. Mol. Cell *6*, 373–384.

Formosa, T. (2002). Changing the DNA landscape: putting a SPN on chromatin. In Protein Complexes that Modify Chromatin, J.L. Workman, ed. (Heidelberg, Germany: Springer-Verlag), pp. 171–201.

Formosa, T., Eriksson, P., Wittmeyer, J., Ginn, J., Yu, Y., and Stillman, D.J. (2001). Spt16-Pob3 and the HMG protein Nhp6 combine to form the nucleosome-binding factor SPN. EMBO J. *20*, 3506–3517.

Formosa, T., Ruone, S., Adams, M.D., Olsen, A.E., Eriksson, P., Yu, Y., Rhoades, A.R., Kaufman, P.D., and Stillman, D.J. (2002). Defects in *SPT16* or *POB3* (yFACT) in *Saccharomyces cerevisiae* cause dependence on the Hir/Hpc pathway: polymerase passage may degrade chromatin structure. Genetics *162*, 1557–1571.

Gambus, A., Jones, R.C., Sanchez-Diaz, A., Kanemaki, M., van Deursen, F., Edmondson, R.D., and Labib, K. (2006). GINS maintains association of Cdc45 with MCM in replisome progression complexes at eukaryotic DNA replication forks. Nat. Cell Biol. *8*, 358–366.

Gietz, R.D., and Sugino, A. (1988). New yeast-*Escherichia coli* shuttle vectors constructed with in vitro mutagenized yeast genes lacking six-base pair restriction sites. Gene *74*, 527–534.

Gunjan, A., Paik, J., and Verreault, A. (2005). Regulation of histone synthesis and nucleosome assembly. Biochimie *87*, 625–635.

Henricksen, L.A., Umbricht, C.B., and Wold, M.S. (1994). Recombinant replication protein A: expression, complex formation, and functional characterization. J. Biol. Chem. *269*, 11121–11132.

Hertel, L., De Andrea, M., Bellomo, G., Santoro, P., Landolfo, S., and Gariglio, M. (1999). The HMG protein T160 colocalizes with DNA replication foci and is down-regulated during cell differentiation. Exp. Cell Res. *250*, 313–328.

Holm, L., and Sander, C. (1998). Touring protein fold space with Dali/FSSP. Nucleic Acids Res. *26*, 316–319.

Iftode, C., Daniely, Y., and Borowiec, J.A. (1999). Replication protein A (RPA): the eukaryotic SSB. Crit. Rev. Biochem. Mol. Biol. *34*, 141–180.

Jacobs, D.M., Lipton, A.S., Isern, N.G., Daughdrill, G.W., Lowry, D.F., Gomes, X., and Wold, M.S. (1999). Human replication protein A: global fold of the N-terminal RPA-70 domain reveals a basic cleft and flexible C-terminal linker. J. Biomol. NMR *14*, 321–331.

John, S., Howe, L., Tafrov, S.T., Grant, P.A., Sternglanz, R., and Workman, J.L. (2000). The something about silencing protein, Sas3, is the catalytic subunit of NuA3, a yTAF(II)30-containing HAT complex that interacts with the Spt16 subunit of the yeast CP (Cdc68/Pob3)-FACT complex. Genes Dev. *14*, 1196–1208.

Kaplan, C.D., Laprade, L., and Winston, F. (2003). Transcription elongation factors repress transcription initiation from cryptic sites. Science *301*, 1096–1099.

Kaufman, P.D., Cohen, J.L., and Osley, M.A. (1998). Hir proteins are required for position-dependent gene silencing in *Saccharomyces cerevisiae* in the absence of chromatin assembly factor I. Mol. Cell. Biol. *18*, 4793–4806.

Keller, D.M., and Lu, H. (2002). p53 serine 392 phosphorylation increases after UV through induction of the assembly of the CK2.hSPT16.SSRP1 complex. J. Biol. Chem. *277*, 50206–50213.

Kim, H.S., and Brill, S.J. (2001). Rfc4 interacts with Rpa1 and is required for both DNA replication and DNA damage checkpoints in *Saccharomyces cerevisiae*. Mol. Cell. Biol. *21*, 3725–3737.

Kim, M., Ahn, S.H., Krogan, N.J., Greenblatt, J.F., and Buratowski, S. (2004). Transitions in RNA polymerase II elongation complexes at the 3′ ends of genes. EMBO J. *23*, 354–364.

Krogan, N.J., Kim, M., Ahn, S.H., Zhong, G., Kobor, M.S., Cagney, G., Emili, A., Shilatifard, A., Buratowski, S., and Greenblatt, J.F. (2002). RNA polymerase II elongation factors of *Saccharomyces cerevisiae*: a targeted proteomics approach. Mol. Cell. Biol. *22*, 6979–6992.

Langst, G., and Becker, P.B. (2004). Nucleosome remodeling: one mechanism, many phenomena? Biochim. Biophys. Acta *1677*, 58–63.

Lemmon, M.A. (2004). Pleckstrin homology domains: not just for phosphoinositides. Biochem. Soc. Trans. *32*, 707–711.

Malone, E.A., Clark, C.D., Chiang, A., and Winston, F. (1991). Mutation in *SPT16/CDC68* suppress *cis*- and *trans*-acting mutations that affect promoter function in *Saccharomyces cerevisiae*. Mol. Cell. Biol. *11*, 5710–5717.

Marchler-Bauer, A., and Bryant, S.H. (2004). CD-Search: protein domain annotations on the fly. Nucleic Acids Res. *32*, W327–W331.

Marchler-Bauer, A., Anderson, J.B., Cherukuri, P.F., DeWeese-Scott, C., Geer, L.Y., Gwadz, M., He, S., Hurwitz, D.I., Jackson, J.D., Ke, Z., et al. (2005). CDD: a Conserved Domain Database for protein classification. Nucleic Acids Res. *33*, D192–D196.

Mason, P.B., and Struhl, K. (2003). The FACT complex travels with elongating RNA polymerase II and is important for the fidelity of transcriptional initiation in vivo. Mol. Cell. Biol. *23*, 8323–8333.

Masse, J.E., Wong, B., Yen, Y.M., Allain, F.H., Johnson, R.C., and Feigon, J. (2002). The *S. cerevisiae* architectural HMGB protein NHP6A complexed with DNA: DNA and protein conformational changes upon binding. J. Mol. Biol. *323*, 263–284.

O'Donnell, A.F., Brewster, N.K., Kurniawan, J., Minard, L.V., Johnston, G.C., and Singer, R.A. (2004). Domain organization of the yeast histone chaperone FACT: the conserved N-terminal domain of FACT subunit Spt16 mediates recovery from replication stress. Nucleic Acids Res. *32*, 5894–5906.

Okuhara, K., Ohta, K., Seo, H., Shioda, M., Yamada, T., Tanaka, Y., Dohmae, N., Seyama, Y., Shibata, T., and Murofushi, H. (1999). A DNA unwinding factor involved in DNA replication in cell-free extracts of xenopus eggs. Curr. Biol. *9*, 341–350.

Orphanides, G., LeRoy, G., Chang, C.-H., Luse, D.S., and Reinberg, D. (1998). FACT, a factor that facilitates transcript elongation through nucleosomes. Cell *92*, 105–116.

Orphanides, G., Wu, W.H., Lane, W.S., Hampsey, M., and Reinberg, D. (1999). The chromatin-specific transcription elongation factor FACT comprises the human SPT16/CDC68 and SSRP1 proteins. Nature *400*, 284–288.

Otwinowski, Z., and Minor, W. (1996). Processing of X-ray diffraction data collected in oscillation mode. Methods Enzymol. *276*, 307–326.

Painter, J., and Merritt, E.A. (2006). TLSMD web server for the generation of multi-group TLS models. J. Appl. Cryst. *39*, 109–111.

Parsons, A.B., Brost, R.L., Ding, H., Li, Z., Zhang, C., Sheikh, B., Brown, G.W., Kane, P.M., Hughes, T.R., and Boone, C. (2004). Integration of chemical-genetic and genetic interaction data links bioactive compounds to cellular target pathways. Nat. Biotechnol. *22*, 62–69.

Pearson, M.A., Reczek, D., Bretscher, A., and Karplus, P.A. (2000). Structure of the ERM protein moesin reveals the FERM domain fold masked by an extended actin binding tail domain. Cell *101*, 259–270.

Ponting, C.P. (2002). Novel domains and orthologues of eukaryotic transcription elongation factors. Nucleic Acids Res. *30*, 3643–3652.

Qian, Z., Huang, H., Hong, J.Y., Burck, C.L., Johnston, S.D., Berman, J., Carol, A., and Liebman, S.W. (1998). Yeast Ty1 retrotransposition is stimulated by a synergistic interaction between mutations in chromatin assembly factor I and histone regulatory proteins. Mol. Cell. Biol. *18*, 4783–4792.

Recht, J., Dunn, B., Raff, A., and Osley, M.A. (1996). Functional analysis of histones H2A and H2B in transcriptional repression in Saccharomyces cerevisiae. Mol. Cell Biol. *16*, 2545–2553.

Rhoades, A.R., Ruone, S., and Formosa, T. (2004). Structural features of nucleosomes reorganized by yeast FACT and its HMG box component, Nhp6. Mol. Cell. Biol. *24*, 3907–3917.

Rowley, A., Singer, R.A., and Johnston, G. (1991). *CDC68*, a yeast gene that affects regulation of cell proliferation and transcription, encodes a protein with a highly acidic carboxyl terminus. Mol. Cell. Biol. *11*, 5718–5726.

Ruone, S., Rhoades, A.R., and Formosa, T. (2003). Multiple Nhp6 molecules are required to recruit Spt16-Pob3 to form yFACT complexes and reorganize nucleosomes. J. Biol. Chem. *278*, 45288–45295.

Saunders, A., Werner, J., Andrulis, E.D., Nakayama, T., Hirose, S., Reinberg, D., and Lis, J.T. (2003). Tracking FACT and the RNA polymerase II elongation complex through chromatin in vivo. Science *301*, 1094–1096.

Schlesinger, M.B., and Formosa, T. (2000). *POB3* is required for both transcription and replication in the yeast *Saccharomyces cerevisiae*. Genetics *155*, 1593–1606.

Shimojima, T., Okada, M., Nakayama, T., Ueda, H., Okawa, K., Iwamatsu, A., Handa, H., and Hirose, S. (2003). Drosophila FACT contributes to Hox gene expression through physical and functional interactions with GAGA factor. Genes Dev. *17*, 1605–1616.

Squazzo, S.L., Costa, P.J., Lindstrom, D., Kumer, K.E., Simic, R., Jennings, J.L., Link, A.J., Arndt, K.M., and Hartzog, G. (2002). The Paf1 complex physically and functionally associates with transcription elongation factors *in vivo*. EMBO J. *21*, 1764–1774.

Terwilliger, T.C. (2003). Automated main-chain model building by template matching and iterative fragment extension. Acta Crystallogr. D Biol. Crystallogr. *59*, 38–44.

Terwilliger, T.C., and Berendzen, J. (1999). Automated MAD and MIR structure solution. Acta Crystallogr. D Biol. Crystallogr. *55*, 849–861.

Vignali, M., Hassan, A.H., Neely, K.E., and Workman, J.L. (2000). ATP-dependent chromatin-remodeling complexes. Mol. Cell. Biol. *20*, 1899–1910.

Wittmeyer, J., and Formosa, T. (1997). The *Saccharomyces cerevisiae* DNA polymerase α catalytic subunit interacts with Cdc68/Spt16 and with Pob3, a protein similar to an HMG1-like protein. Mol. Cell. Biol. *17*, 4178–4190.

Wittmeyer, J., Joss, L., and Formosa, T. (1999). Spt16 and Pob3 of *Saccharomyces cerevisiae* form an essential, abundant heterodimer that is nuclear, chromatin-associated, and copurifies with DNA polymerase α. Biochemistry *38*, 8961–8971.

Yoon, H.S., Hajduk, P.J., Petros, A.M., Olejniczak, E.T., Meadows, R.P., and Fesik, S.W. (1994). Solution structure of a pleckstrin-homology domain. Nature *369*, 672–675.

Yu, J.W., Mendrola, J.M., Audhya, A., Singh, S., Keleti, D., DeWald, D.B., Murray, D., Emr, S.D., and Lemmon, M.A. (2004). Genome-wide analysis of membrane targeting by *S. cerevisiae* pleckstrin homology domains. Mol. Cell *13*, 677–688.

Zhang, W., Bone, J.R., Edmondson, D.G., Turner, B.M., and Roth, S.Y. (1998). Essential and redundant functions of histone acetylation revealed by mutation of target lysines and loss of the Gcn5p acetyltransferase. EMBO J. *17*, 3155–3167.

Zhou, Y., and Wang, T.S. (2004). A coordinated temporal interplay of nucleosome reorganization factor, sister chromatin cohesion factor, and DNA polymerase α facilitates DNA replication. Mol. Cell. Biol. *24*, 9568–9579.

Zou, L., and Elledge, S.J. (2003). Sensing DNA damage through ATRIP recognition of RPA-ssDNA complexes. Science *300*, 1542–1548.

Accession Numbers

Protein Data Bank entry codes are 2GCL for wild-type Pob3-M and 2GCJ for the Q308K mutant.

Supplemental Data

The Structure of the yFACT Pob3-M Domain,

Its Interaction with the DNA Replication Factor

RPA, and a Potential Role in Nucleosome Deposition

Andrew P. VanDemark, Mary Blanksma, Elliott Ferris, Annie Heroux, Christopher P. Hill, and Tim Formosa

Table S1. Strains Used

Isogenic with A364a	
8127-5-2	*MATα ura3-Δ0 leu2-Δ0 trp1-Δ2 his3 lys2-128∂*
8127-7-4	*MATa ura3-Δ0 leu2-Δ0 trp1-Δ2 his3 lys2-128∂*
8136-F133S	*MATa ura3-Δ0 leu2-Δ0 trp1-Δ2 his3 lys2-128∂ pob3-F133S*
8136-Q308K	*MATa ura3-Δ0 leu2-Δ0 trp1-Δ2 his3 lys2-128∂ pob3-Q308K*
8151-1-1	*MATa ura3-Δ0 leu2-Δ0 trp1-Δ2 his7 lys2-128∂*
8151-1-2	*MATa ura3-Δ0 leu2-Δ0 trp1-Δ2 his7 lys2-128∂ pob3-Q308K*
8151-1-3	*MATα ura3-Δ0 leu2-Δ0 trp1-Δ2 his3 lys2-128∂ pob3-Q308K*
8153-2-1a	*MATa ura3-Δ0 leu2-Δ0 trp1-Δ2 his7 lys2-128∂ pob3-Q308K, T311A*
8153-6-7a	*MATa ura3-Δ0 leu2-Δ0 trp1-Δ2 his3 lys2-128∂ rfa1-A88P*
8208-2-2	*MATα ura3-Δ0 leu2-Δ0 trp1-Δ2 his3 lys2-128∂ rfa1-A88P*
8208-7-2	*MATa ura3-Δ0 leu2-Δ0 trp1-Δ2 his7 lys2-128∂ rfa1-A88P*
8208-7-3	*MATα ura3-Δ0 leu2-Δ0 trp1-Δ2 his3 lys2-128∂ pob3-Q308K(URA3) rfa1-A88P*
8212-3-2	*MATa ura3-Δ0 leu2-Δ0 trp1-Δ2 his3 lys2-128∂ pob3-F133S rfa1-A88P*
8213-10-2	*MATa ura3 leu2 trp1 his3 pob3-2 lys2-128∂ rfa1-A88P*
8213-4-1	*MATa ura3 leu2 trp1 his3 pob3-2 lys2-128∂*
8216-3-3	*MATα ura3 leu2 trp1 his3 rad53/mec2-1(URA3) lys2-128∂ pob3-Q308K*
8216-9-1	*MATα ura3 leu2 trp1 his7 rad53/mec2-1(URA3) lys2-128∂*
8217-2-1	*MATa ura3 leu2 trp1 his3 lys2-128∂ rlf2/cac1-Δ(::LEU2) pob3-Q308K(URA3)*
8217-6-2	*MATa ura3 leu2 trp1 his3 lys2-128∂ rlf2/cac1-Δ(::LEU2)*
8218-2-4	*MATa ura3-Δ0 leu2-Δ0 trp1-Δ2 his3 lys2-128∂ hta2-htb2-Δ(::HIS3)*
8218-3-3	*MATa ura3-Δ0 leu2-Δ0 trp1-Δ2 his3 lys2-128∂ pob3-Q308K (URA3) hta2-htb2-Δ(::HIS3)*
8219-3-3	*MATa ura3-Δ0 leu2-Δ0 trp1-Δ2 his3 lys2-128∂ hht1-hhf1-Δ(::TRP1)*
8219-10-1	*MATa ura3-Δ0 leu2-Δ0 trp1-Δ2 his3 lys2-128∂ pob3-Q308K(URA3) hht1-hhf1-Δ(::TRP1)*
8239	*MATa ura3-Δ0 leu2-Δ0 trp1-Δ2 lys2-128∂ his3 rfa1-A88P hht1-hhf1-Δ(::LEU2) hht2-hhf2-Δ(::KanMX) DS1700 (YCp URA3 HHT2-HHF2)*
8244-13-2	*MATα ura3-Δ0 leu2-Δ0 trp1-Δ2 his3 lys2-128∂ hht1-hhf1-Δ(::LEU2) hht2-hhf2-Δ(::KanMX) DS1700 (YCp URA3 HHT2-HHF2)*
8244-18-4	*MATα ura3-Δ0 leu2-Δ0 trp1-Δ2 his7 lys2-128∂ hht1-hhf1-Δ(::LEU2) hht2-hhf2-Δ(::KanMX) pob3-Q308K DS1700 (YCp URA3 HHT2-HHF2)*

Isogenic with W303	
DY2861	*MATα ade2(his4-912∂) can1 leu2 trp1 ura3 his4-912∂ lys2-128∂*
8224	*MATα ade2(his4-912∂) can1 leu2 trp1 ura3 his4-912∂ lys2-128∂ pob3-Q308K*
8230-1-3	*MATα ade2 can1 his3 leu2 lys2-128∂ trp1 ura3 rpd3-Δ(::LEU2) pob3-Q308K*
8230-2-1	*MATα ade2 can1 leu2 lys2-128∂ trp1 ura3 rpd3-Δ(::LEU2) his4-912∂*
8230-2-4	*MATα ade2(his4-912∂) can1 leu2 lys2 trp1 ura3 gcn5-Δ(::TRP1) his4-912∂ pob3-Q308K*
8230-9-2	*MATα ade2(his4-912∂) can1 leu2 lys2 trp1 ura3 gcn5-Δ(::TRP1) his4-912∂*
Hybrid	
7787-4-4 pTF138	*MATa ura3 leu2 trp1 his4-912∂ lys2-128∂ pob3-Δ(::TRP1) pTF138 (YEp URA3 POB3)*

Strains are isogenic with the A364a or W303 backgrounds as indicated, except 7787-4-4, a hybrid used only during the screen for *pob3* alleles to compare the effects of mutated plasmids to one another. *pob3-Q308K(URA3)* has the *URA3* gene inserted 34 bp downstream of the *POB3* ORF; this marker does not affect the HU sensitivity or other phenotypes caused by the Q308K mutation. *ade2(his4-912∂)* has the promoter from the Spt$^-$ reporter *his4-912∂* driving the *ADE2* gene.

Figure1-Supplemental

A

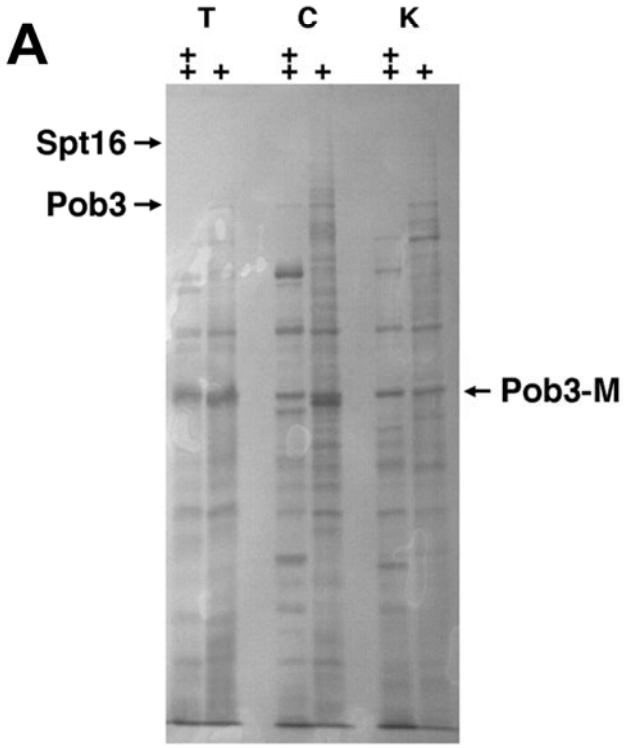

B

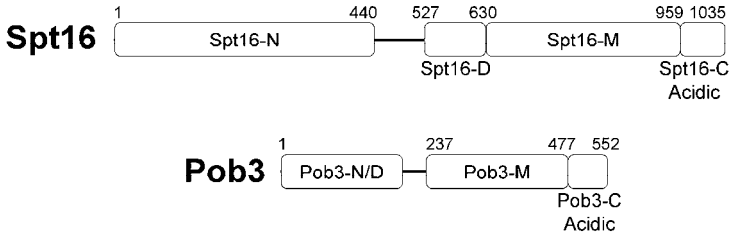

C

Pob3 Fragment	Spt16 Fragment	Co-Purify
Pob3-N/D — Pob3-M — C	Spt16-N — D — Spt16-M — C	Yes
Pob3-N/D — Pob3-M	D — Spt16-M — C	Yes
Pob3-N/D	D — Spt16-M — C	Yes
Pob3-M	D — Spt16-M — C	No
Pob3-N/D	Spt16-N	No
Pob3-N/D	D — Spt16-M	Yes
Pob3-N/D	D	Yes
Pob3-N/D	D — Spt16-M — C	Yes
Pob3-N/D	Spt16-M — C	No

Figure S1. Determining the Structural Domains of Spt16-Pob3

(A) Purified Spt16-Pob3 was digested with dilutions of trypsin (T), chymotrypsin (C) or proteinase K (K) then the fragments generated by partial digestion were separated by SDS-PAGE, transferred to PVDF membrane (ProBlott, Applied Biosystems), and sequenced by Edman degradation. Sequences revealed digestion of Pob3 by trypsin after K218 and K231, by chymotrypsin after A214, and by proteinase K after F224. The sizes of the fragments recovered with N-termini generated by these proteolytic cuts suggested that the acidic C-terminal tail domain could also be removed, leaving a protease-resistant 30 kDa fragment representing the central Pob3-M domain indicated. Bands identified as fragments of Spt16 by Western blotting of the same samples did not yield unambiguous protein sequences and could therefore either be from the N-terminus of Spt16, which is known to be blocked, or could result from multiple products migrating as a single band. The major protease-resistant bands derived from Spt16 were consistent with the sizes expected for Spt16-N and Spt16-M.

(B) Schematic representation of the domain structure of Spt16-Pob3 incorporating the results from panels A and C. The residue numbers listed indicate the approximate boundaries of the structural domains, with the naming convention described in Fig 1 of the main text.

(C) Fragments of Spt16 and Pob3 suggested by limited proteolysis were expressed in *E.coli* and the fraction remaining soluble after lysis of the cells and centrifugation was determined. Soluble fragments of Pob3 were then expressed with an 8-histidine tag at their N-termini, and co-purification of co-expressed untagged Spt16 fragments was tested using nickel chelation chromatography (NTA Agarose, Qiagen). The full-length Spt16-Pob3 complex was also purified using this strategy, except the expression was performed in yeast cells and Pob3 was tagged with 12 histidines. Co-purification of Spt16 fragments via the tagged Pob3 is indicated in the last column.

Figure S2

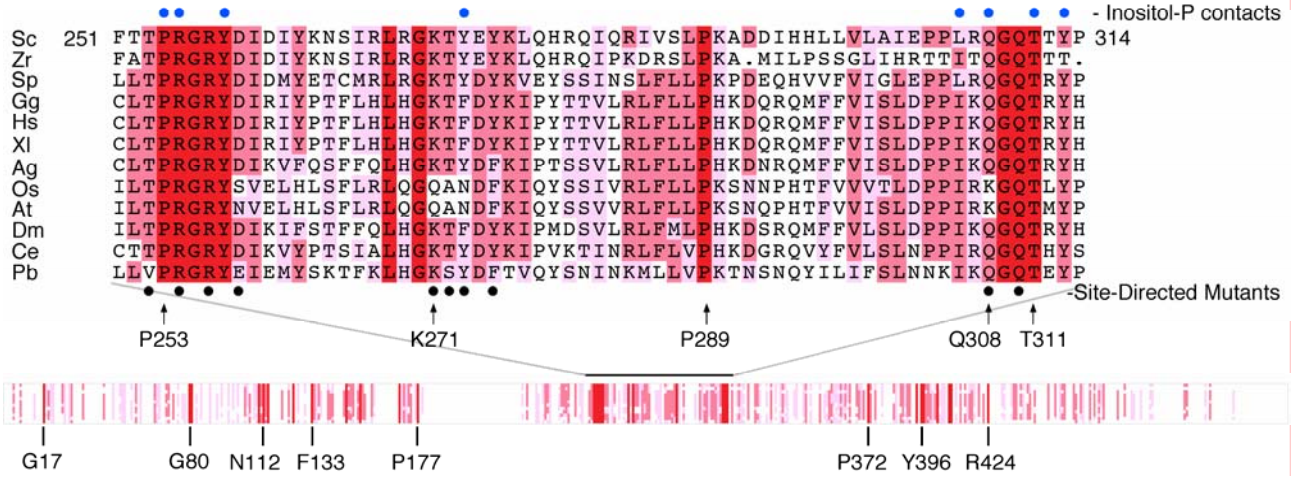

Figure S2. Homology among Members of the Pob3/SSRP1 Family

A BLAST search of GenBank (Altschul et al., 1997) produced about 60 full length sequences with strong similarity to Pob3. 12 proteins distributed over the range of the similarity scores were aligned using Clustal X (Jeanmougin et al., 1998) and shaded according to the degree of conservation. Red indicates 100% identity (12/12), pink indicates identity among 9-11 sequences, and light pink indicates similarity of the residues. The positions of residues that contact inositol phosphate in Pleckstrin (Yoon et al., 1994) are indicated above the alignment. The residues chosen for site-directed mutagenesis as described in the text are indicated below the alignment. The top panel shows the aligned residues in the most highly conserved segment of Pob3 (251-314). The bottom panel shows the shading only for the whole length of Pob3, with selected invariant residues labeled. The proteins compared and their GenBank accession numbers are : *Saccharomyces cerevisiae* (6323571), *Zygosaccharomyces rouxii* (10179001), *Schizosaccharomyces pombe* (4160575), *Gallus gallus* (57524786), *Homo sapiens* (13477285), *Xenopus laevis* (4586285), *Anopheles gambiae* 58393644, *Oryza sativa* (9558422), *Arabidopsis thaliana* (26454672), *Drosophila melanogaster* (12644386), *Caenorhabditis elegans* (1947000), and *Plasmodium berghei* (56492088). Underlined names indicate members of pfam03531 SSrecog--PSSM-Id 23462 (Marchler-Bauer et al., 2005).

Fig S3

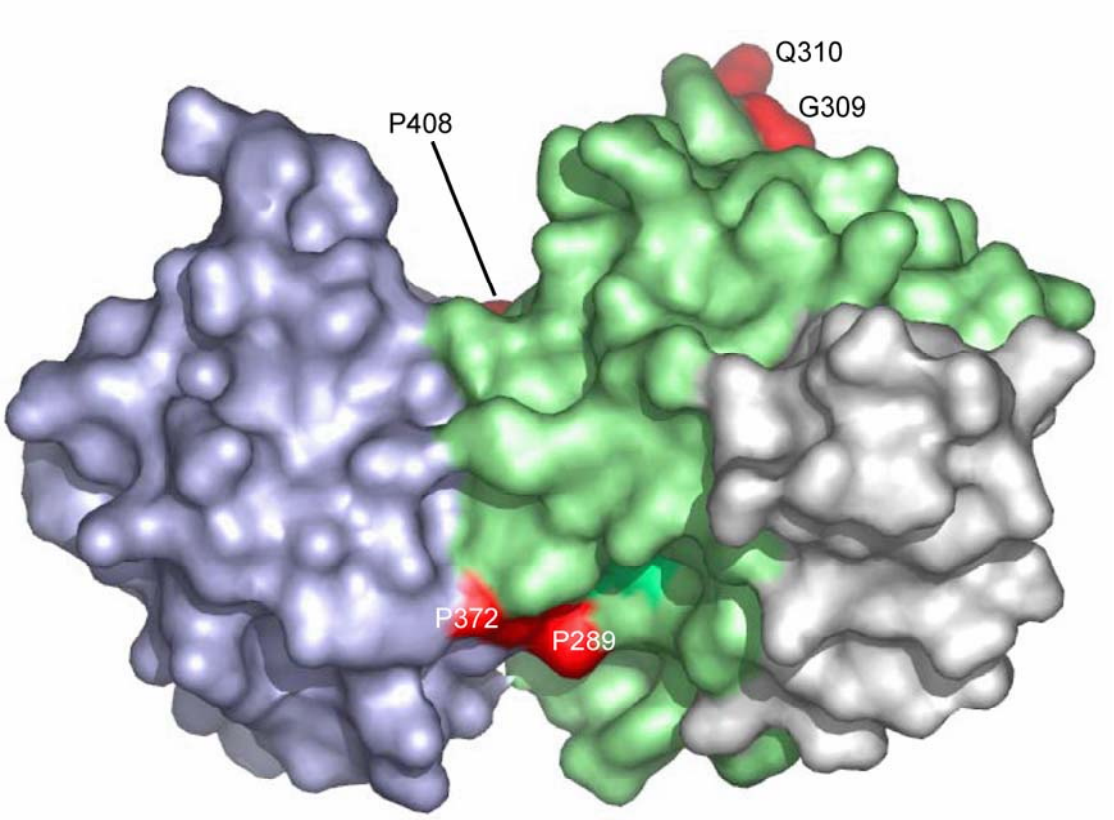

Figure S3. Bottom View of the Pob3-M Surface, Colored as in Figure 2 and Rotated ~180 Degrees from Its Orientation in Figure 2

Shown in red and labeled are invariant residues P289 and P372, which are located next to each other near the interface of the two PH domains. These are the only two invariant residues not visible in Fig 2.

Figure S4

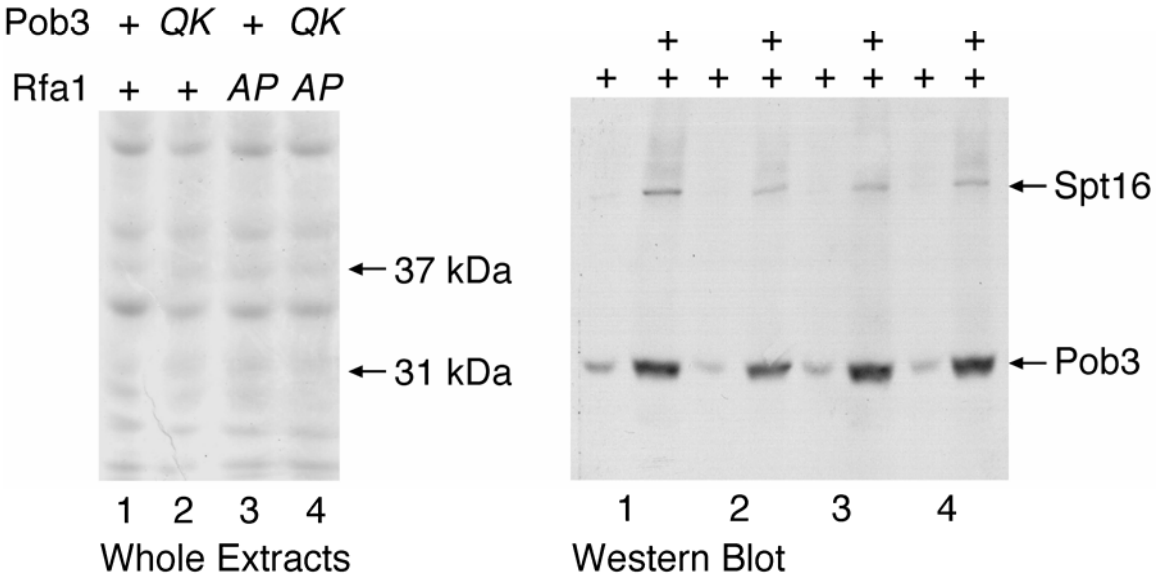

Figure S4. Pob3-Q308K Protein Is Stable in Yeast Cells

Isogenic strains with *pob3-Q308K* (*QK*), *rfa1-A88P* (*AP*), or both mutations as indicated were grown to log phase at 30° C, harvested by centrifugation, then suspended in SDS sample buffer and heated to 65° C for one hour. (Top) Extract representing 2.5 X 10^6 cells was subjected to SDS-PAGE on a 7.5% polyacrylamide gel and the gel was stained with Coomassie Blue dye. The region from about 25-50 kDa is shown. Strain 1 (WT) has slightly more total protein than the mutants in lanes 2-4. (Bottom) Aliquots of the same extracts (1-4 in the top panel) but representing 10^6 cells (+) or 5 X 10^6 cells (++) were subjected to SDS-PAGE, transferred to nitrocellulose (Schleicher and Schuell BA83), probed with antisera generated against Spt16 and Pob3, and detected by ECL (Amersham Biosciences). The signals for Spt16 and Pob3 relative to the total amount of protein loaded are equivalent for all four strains, indicating the overall stability of the Spt16-Pob3 complexes in all four genetic combinations under the conditions used to assess HU sensitivity.

Figure S5

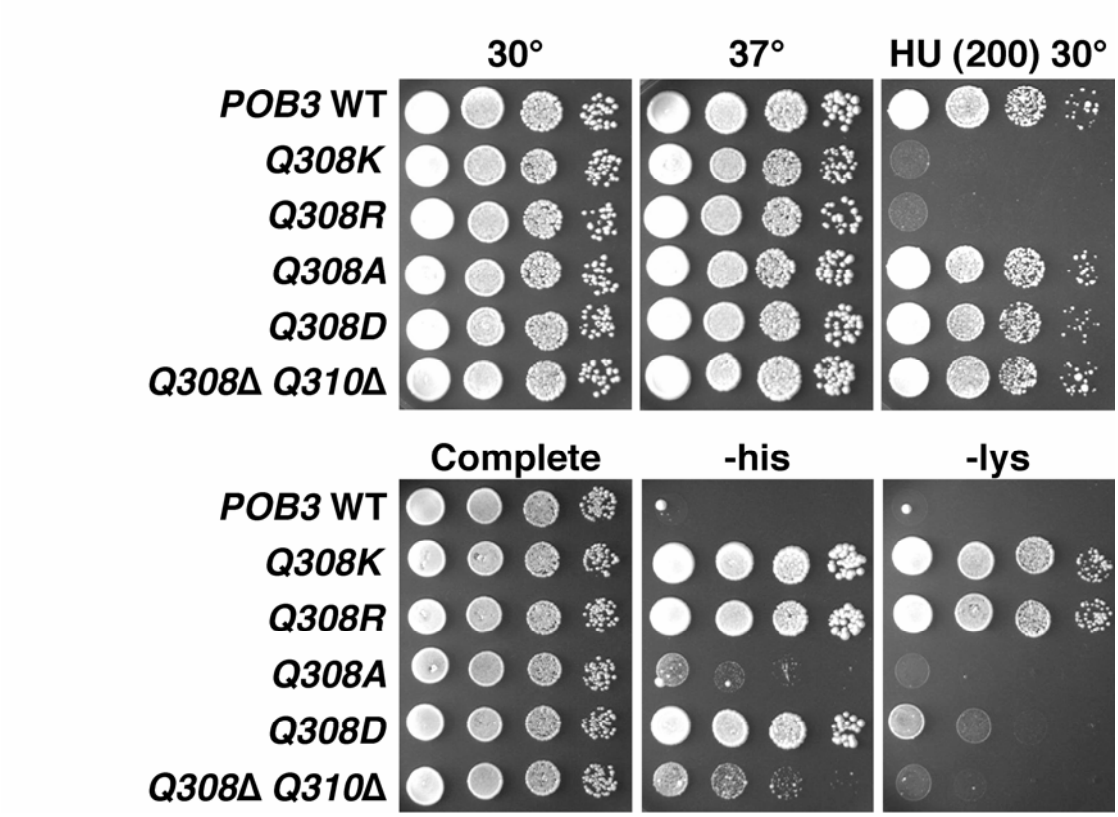

Figure S5. Phenotypes Caused by Mutations in and near Pob3-Q308

Strain 7787-4-4 pTF138 (*pob3*-Δ YEp *URA3 POB3*) was transformed with derivatives of pTF139 (YCp *LEU2 POB3*) with the *POB3* allele shown. Strains free of pTF138 were obtained by selection on medium containing 5-FOA, then cultures were grown in rich medium and aliquots of 10-fold serial dilutions were placed on rich medium with or without 200 mM HU and incubated at the temperature indicated (top panels). Only Q308K and Q308R alleles were found in the screen for HU sensitivity, but this might have meant that only these substitutions cause this phenotype, only these mutations are common, or that these are the only substitutions at this site that support viability. These results show that other residues are tolerated but do not cause the HU sensitivity observed with Q308K/R. (Bottom panels) Aliquots were also placed on complete synthetic media or media lacking histidine or lysine and incubated at 30° to measure the Spt$^-$ phenotype. *pob3-Q308K* and *pob3-Q308R* caused a robust Spt$^-$ phenotype (rapid growth on medium lacking lysine). *pob3-Q308D*, which did not cause sensitivity to HU, caused a significant transcription defect (good growth on –his but not on –lys; *lys2-128∂* is a more stringent reporter of the Spt- phenotype than *his4-912∂* as noted in Simchen et al., 1984). *pob3-Q308*Δ *Q310*Δ, an allele completely lacking

residues 308 and 310, caused only a very mild Spt$^-$ phenotype, producing weak growth on –his only after extended incubation. *pob3-Q308A* caused little or no effect. Neither the residue at position 308 nor the length of the loop containing it are therefore necessary for the normal function of *POB3* in promoting resistance to HU, but substitution with a basic residue blocks this function. Substitution with an acidic residue causes a defect in transcription, but not a defect in replication.

Figure S6

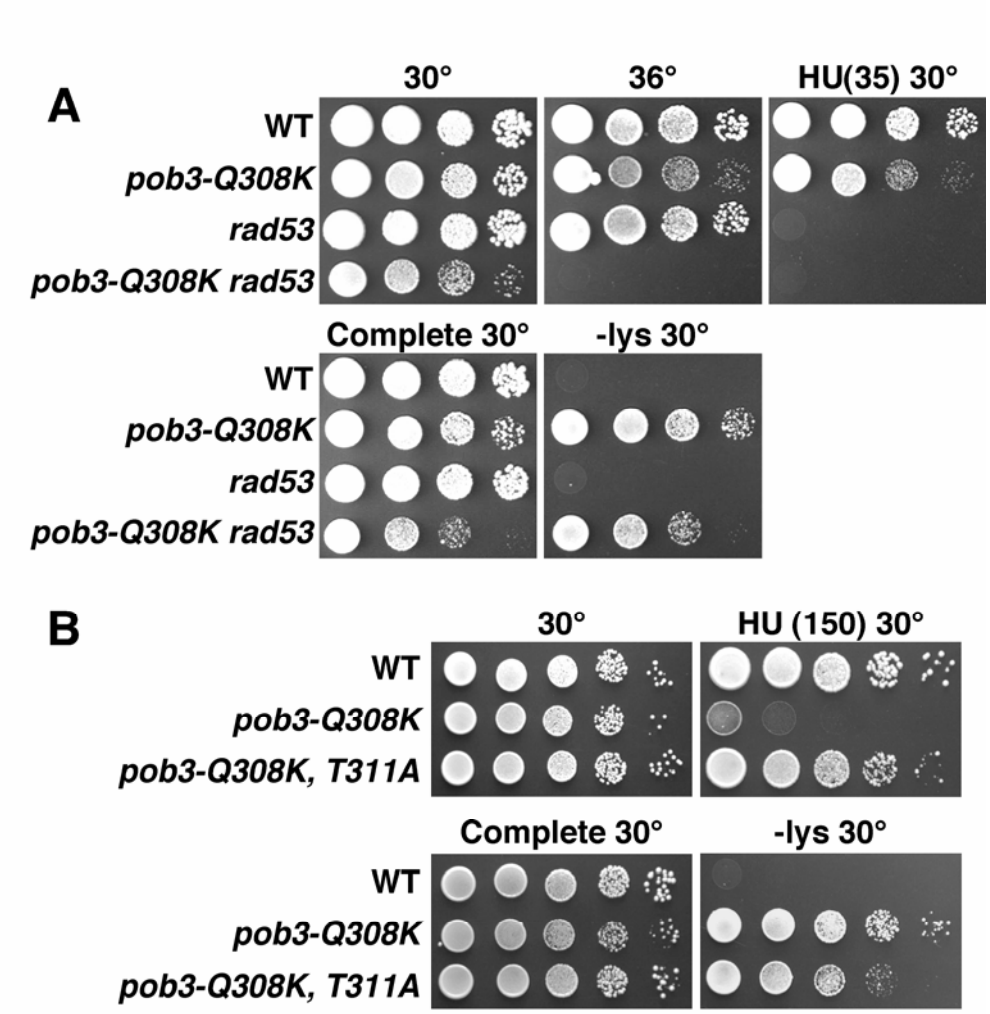

Figure S6. Effect of Combining a *pob3-Q308K* Mutation with a Checkpoint Defect or with an Intragenic Suppressor Mutation

(A) Isogenic strains 8127-5-2 (WT), 8151-1-3 (pob3-Q308K), 8216-9-1 (rad53), and 8216-3-3 (pob3-Q308K rad53) were processed as above, and placed on rich medium with or without 35 mM HU (top panels) or on synthetic medium with or without lysine (bottom panels), then incubated at the temperature indicated. The rad53 mutation caused a severe growth defect when combined with *pob3-Q308K*, leading to slow growth at 30° and strong temperature sensitivity at 36°, a temperature permissive for either single mutant. The rad53 mutation causes much more severe sensitivity to HU than *pob3-Q308K* does, so the effect of combining the mutations was not detectable at concentrations of HU as low as 20 mM (data not shown). However, no evidence for suppression of

HU sensitivity was evident. The growth defect of the double mutant does not appear to be due to an increased defect in transcription, as both the *pob3-Q308K* strain and the double mutant have about the same level of Spt$^-$ phenotype (about the same growth rate for each strain comparing growth on complete to –lys medium). This shows that the mutual suppression of the DNA replication defect observed in *rfa1-A88P pob3-Q308K* double mutants cannot be recapitulated by inactivating the DNA damage checkpoint another way, and that the viability of *pob3-Q308K* mutants depends on *RAD53*, consistent with the *pob3-Q308K* defect causing the equivalent of DNA damage.

(B) Isogenic strains 8151-1-1 (WT), 8151-1-2 (*pob3-Q308K*), and 8153-2-1a (*pob3-Q308K, T311A*) were processed as above and placed on rich (top panels) or synthetic (bottom panels) medium. The T311A mutation suppresses the HU sensitivity caused by *pob3-Q308K* efficiently, but the strain is still Spt$^-$ (Lys$^+$). As with *rfa1-A88P*, this shows that the replication and transcription defects caused by *pob3-Q308K* are genetically separable, with essentially complete suppression of the HU sensitivity being accompanied by a minimal change in the Spt$^-$ phenotype.

Supplemental References

Altschul, S. F., Madden, T. L., Schaffer, A. A., Zhang, J., Zhang, Z., Miller, W., and Lipman, D. J. (1997). Gapped BLAST and PSI-BLAST: a new generation of protein database search programs. Nucleic Acids Res *25*, 3389-3402.

Collaborative Computational Project, N. (1994). The CCP4 suite: programs for protein crystallography. Acta Crystallogr D Biol Crystallogr *50*, 760-763.

Emsley, P., and Cowtan, K. (2004). Coot: model-building tools for molecular graphics. Acta Crystallogr D Biol Crystallogr *60*, 2126-2132.

Gietz, R. D., and Sugino, A. (1988). New yeast-*Escherichia coli* shuttle vectors constructed with in vitro mutagenized yeast genes lacking six-base pair restriction sites. Gene *74*, 527-534.

Henricksen, L. A., Umbricht, C. B., and Wold, M. S. (1994). Recombinant replication protein A: expression, complex formation, and functional characterization. J Biol Chem *269*, 11121-11132.

Jeanmougin, F., Thompson, J. D., Gouy, M., Higgins, D. G., and Gibson, T. J. (1998). Multiple sequence alignment with Clustal X. Trends Biochem Sci *23*, 403-405.

Marchler-Bauer, A., Anderson, J. B., Cherukuri, P. F., DeWeese-Scott, C., Geer, L. Y., Gwadz, M., He, S., Hurwitz, D. I., Jackson, J. D., Ke, Z.*, et al.* (2005). CDD: a Conserved Domain Database for protein classification. Nucleic Acids Res *33*, D192-196.

Otwinowski, Z., and Minor, W. (1996). Processing of X-ray diffraction data collected in oscillation mode. Methods Enzymol *276*, 307-326.

Painter, J., and Merritt, E. A. (2006). TLSMD web server for the generation of multi-group TLS models. J Appl Cryst *39*, 109-111.

Rhoades, A. R., Ruone, S., and Formosa, T. (2004). Structural features of nucleosomes reorganized by yeast FACT and its HMG box component, Nhp6. Mol Cell Biol *24*, 3907-3917.

Schlesinger, M. B., and Formosa, T. (2000). POB3 is required for both transcription and replication in the yeast Saccharomyces cerevisiae. Genetics *155*, 1593-1606.

Simchen, G., Winston, F., Styles, C. A., and Fink, G. R. (1984). Ty-mediated gene expression of the LYS2 and HIS4 genes of Saccharomyces cerevisiae is controlled by the same SPT genes. Proc Natl Acad Sci U S A *81*, 2431-2434.

Terwilliger, T. C. (2003). Automated main-chain model building by template matching and iterative fragment extension. Acta Crystallogr D Biol Crystallogr *59*, 38-44.

Terwilliger, T. C., and Berendzen, J. (1999). Automated MAD and MIR structure solution. Acta Crystallogr D Biol Crystallogr *55 (Pt 4)*, 849-861.

Yoon, H. S., Hajduk, P. J., Petros, A. M., Olejniczak, E. T., Meadows, R. P., and Fesik, S. W. (1994). Solution structure of a pleckstrin-homology domain. Nature *369*, 672-675.